

Generalized-Ensemble Algorithms for Protein Folding Simulations

Yuji Sugita,^{a,1} Ayori Mitsutake,^{b,2} and Yuko Okamoto^{c,3}

^a*Theoretical Biochemistry Laboratory
Discovery Research Institute, RIKEN
Wako-shi, Saitama 351-0198, Japan*

^b*Department of Physics, Keio University
Yokohama, Kanagawa 223-8522, Japan*

^c*Department of Physics, Nagoya University
Nagoya, Aichi 464-8602, Japan*

To appear in *Lecture Notes in Physics
Rugged Free Energy Landscapes: Common Computational Approaches
to Spin Glasses, Structural Glasses and Biological Macromolecules*,
W. Janke (ed.) (Springer-Verlag)

ABSTRACT

Conventional simulations of complex systems in the canonical ensemble suffer from the quasi-ergodicity problem. A simulation in generalized ensemble overcomes this difficulty by performing a random walk in potential energy space and other parameter space. From only one simulation run, one can obtain canonical-ensemble averages of physical quantities as functions of temperature by the single-histogram and/or multiple-histogram reweighting techniques. In this article we review the generalized-ensemble algorithms. Three well-known methods, namely, multicanonical algorithm, simulated tempering, and replica-exchange method, are described first. Both Monte Carlo and molecular dynamics versions of the algorithms are given. We then present further extensions of the above three methods.

1 INTRODUCTION

Canonical fixed-temperature simulations of complex systems such as spin glasses and biopolymers are greatly hampered by the multiple-minima problem, or the quasi-ergodicity problem. Because simulations at low temperatures tend to get trapped in a few of a huge number of local-minimum-energy states which are separated by high energy barriers, it is very difficult to obtain accurate canonical distributions at low temperatures by conventional Monte Carlo (MC) and molecular dynamics (MD) methods. One way to overcome this multiple-minima problem is to perform a simulation in a *generalized ensemble* where each state is weighted by an artificial, non-Boltzmann probability weight factor so that a

¹ e-mail: sugita@riken.jp

² e-mail: ayori@rk.phys.keio.ac.jp

³ e-mail: okamoto@phys.nagoya-u.ac.jp

random walk in potential energy space may be realized (for reviews see, e.g., Refs. [1]–[7]). The random walk allows the simulation to escape from any energy barrier and to sample much wider configurational space than by conventional methods. Monitoring the energy in a single simulation run, one can obtain not only the global-minimum-energy state but also canonical ensemble averages as functions of temperature by the single-histogram [8] and/or multiple-histogram [9, 10] reweighting techniques (an extension of the multiple-histogram method is also referred to as *weighted histogram analysis method* (WHAM) [10]). Besides generalized-ensemble algorithms, which are usually based on local updates, methods based on non-local updates such as cluster algorithms and their generalizations have also been widely used [11]–[13]. In this article, we focus our discussion on generalized-ensemble algorithms.

One of the most well-known generalized-ensemble methods is perhaps *multicanonical algorithm* (MUCA) [14, 15] (for reviews see, e.g., Refs. [16, 17]). (The method is also referred to as *entropic sampling* [18] and *adaptive umbrella sampling* [19] of the potential energy [20]. MUCA can also be considered as a sophisticated, ideal realization of a class of algorithms called *umbrella sampling* [21]. Also closely related methods are *transition matrix methods* reviewed in Refs. [22, 4] and *random walk algorithm* [23, 24], which is also referred to as *density of states Monte Carlo* [25]. See also Ref. [26].) MUCA and its generalizations have been applied to spin systems (see, e.g., Refs. [27]–[32]). MUCA was also introduced to the molecular simulation field [33]. Since then MUCA and its generalizations have been extensively used in many applications in protein and related systems [34]–[64]. Molecular dynamics version of MUCA has also been developed [41, 44, 20] (see also Refs. [65, 41] for Langevin dynamics version). MUCA has been extended so that flat distributions in other parameters instead of potential energy may be obtained [28, 29, 40, 45, 47, 62]. Moreover, multidimensional (or multicomponent) extensions of MUCA can be found in Refs. [40, 45, 46, 64].

While a simulation in multicanonical ensemble performs a free 1D random walk in potential energy space, that in *simulated tempering* (ST) [66, 67] (the method is also referred to as the *method of expanded ensemble* [66]) performs a free random walk in temperature space (for a review, see, e.g., Ref. [68]). This random walk, in turn, induces a random walk in potential energy space and allows the simulation to escape from states of energy local minima. ST has also been applied to protein folding problem [69, 42, 43, 70].

The generalized-ensemble algorithms are powerful, but in the above two methods the probability weight factors are not *a priori* known and have to be determined by iterations of short trial simulations. This process can be non-trivial and very tedious for complex systems with many degrees of freedom. Therefore, there have been attempts to accelerate the convergence of the iterative process for MUCA weight factor determination [27, 40, 71, 72, 73, 20] (see also Refs. [16, 74]).

In the *replica-exchange method* (REM) [75]–[77], the difficulty of weight factor determination is greatly alleviated. (A closely related method was independently developed in Ref. [78]. Similar methods in which the same equations are used but emphasis is laid on optimizations have been developed [79, 80]. REM is also referred to as *multiple Markov chain method* [81] and *parallel tempering* [68]. Details of literature about REM and related algorithms can be found in recent reviews [82, 2].) In this method, a number of non-interacting copies (or replicas) of the original system at different temperatures are simulated independently and simultaneously by the conventional MC or MD method. Every few steps, pairs of replicas are exchanged with a specified transition probability. The

weight factor is just the product of Boltzmann factors, and so it is essentially known.

REM has already been used in many applications in protein systems [83, 84, 70][85]–[97]. Other molecular simulation fields have also been studied by this method in various ensembles [98]–[103]. Moreover, REM was applied to cluster studies in quantum chemistry field [104]. The details of molecular dynamics algorithm have been worked out for REM in Ref. [84] (see also Refs. [83, 101]). This led to a wide application of replica-exchange molecular dynamics method in the protein folding problem [105]–[112].

However, REM also has a computational difficulty: As the number of degrees of freedom of the system increases, the required number of replicas also greatly increases, whereas only a single replica is simulated in MUCA or ST. This demands a lot of computer power for complex systems. Our solution to this problem is: Use REM for the weight factor determinations of MUCA or ST, which is much simpler than previous iterative methods of weight determinations, and then perform a long MUCA or ST production run. The first example is the *replica-exchange multicanonical algorithm* (REMUCA) [88, 93, 94]. In REMUCA, a short replica-exchange simulation is performed, and the multicanonical weight factor is determined by the multiple-histogram reweighting techniques [9, 10]. Another example of such a combination is the *replica-exchange simulated tempering* (REST) [89]. In REST, a short replica-exchange simulation is performed, and the simulated tempering weight factor is determined by the multiple-histogram reweighting techniques [9, 10].

We have introduced two further extensions of REM, which we refer to as *multicanonical replica-exchange method* (MUCAREM) [88, 93, 94] (see also Refs. [113, 114]) and *simulated tempering replica-exchange method* (STREM) [115] (see also Ref. [116] for a similar idea). In MUCAREM, a replica-exchange simulation is performed with a small number of replicas each in multicanonical ensemble of different energy ranges. In STREM, on the other hand, a replica-exchange simulation is performed with a small number of replicas in “simulated tempering” ensemble of different temperature ranges.

Finally, one is naturally led to a multidimensional (or, multivariable) extension of REM, which we refer to as *multidimensional replica-exchange method* (MREM) [86] (see also Refs. [117, 99, 118, 112, 119]). A special realization of MREM is *replica-exchange umbrella sampling* (REUS) [86] and it is particularly useful in free energy calculations (see also Ref. [87] for a similar idea).

In this article, we describe the generalized-ensemble algorithms mentioned above. Namely, we first review the three familiar methods: MUCA, ST, and REM. We then present further extensions of the three methods.

2 GENERALIZED-ENSEMBLE ALGORITHMS

2.1 Multicanonical Algorithm and Simulated Tempering

Let us consider a system of N atoms of mass m_k ($k = 1, \dots, N$) with their coordinate vectors and momentum vectors denoted by $q \equiv \{\mathbf{q}_1, \dots, \mathbf{q}_N\}$ and $p \equiv \{\mathbf{p}_1, \dots, \mathbf{p}_N\}$, respectively. The Hamiltonian $H(q, p)$ of the system is the sum of the kinetic energy $K(p)$ and the potential energy $E(q)$:

$$H(q, p) = K(p) + E(q) , \quad (1)$$

where

$$K(p) = \sum_{k=1}^N \frac{\mathbf{p}_k^2}{2m_k} . \quad (2)$$

In the canonical ensemble at temperature T each state $x \equiv (q, p)$ with the Hamiltonian $H(q, p)$ is weighted by the Boltzmann factor:

$$W_B(x; T) = \exp(-\beta H(q, p)) , \quad (3)$$

where the inverse temperature β is defined by $\beta = 1/k_B T$ (k_B is the Boltzmann constant). The average kinetic energy at temperature T is then given by

$$\langle K(p) \rangle_T = \left\langle \sum_{k=1}^N \frac{\mathbf{p}_k^2}{2m_k} \right\rangle_T = \frac{3}{2} N k_B T . \quad (4)$$

Because the coordinates q and momenta p are decoupled in Eq. (1), we can suppress the kinetic energy part and can write the Boltzmann factor as

$$W_B(x; T) = W_B(E; T) = \exp(-\beta E) . \quad (5)$$

The canonical probability distribution of potential energy $P_B(E; T)$ is then given by the product of the density of states $n(E)$ and the Boltzmann weight factor $W_B(E; T)$:

$$P_B(E; T) \propto n(E) W_B(E; T) . \quad (6)$$

Since $n(E)$ is a rapidly increasing function and the Boltzmann factor decreases exponentially, the canonical ensemble yields a bell-shaped distribution which has a maximum around the average energy at temperature T . The conventional MC or MD simulations at constant temperature are expected to yield $P_B(E; T)$. A MC simulation based on the Metropolis algorithm [120] is performed with the following transition probability from a state x of potential energy E to a state x' of potential energy E' :

$$w(x \rightarrow x') = \min \left(1, \frac{W_B(E'; T)}{W_B(E; T)} \right) = \min(1, \exp(-\beta \Delta E)) . \quad (7)$$

where

$$\Delta E = E' - E . \quad (8)$$

A MD simulation, on the other hand, is based on the following Newton equations of motion:

$$\dot{\mathbf{q}}_k = \frac{\mathbf{p}_k}{m_k} , \quad (9)$$

$$\dot{\mathbf{p}}_k = -\frac{\partial E}{\partial \mathbf{q}_k} = \mathbf{f}_k , \quad (10)$$

where \mathbf{f}_k is the force acting on the k -th atom ($k = 1, \dots, N$). This set of equations actually yield the microcanonical ensemble, and we have to add a thermostat in order to obtain the

canonical ensemble at temperature T . Here, we just follow Nosé’s prescription [121, 122], and we have

$$\dot{\mathbf{q}}_k = \frac{\mathbf{p}_k}{m_k} , \quad (11)$$

$$\dot{\mathbf{p}}_k = -\frac{\partial E}{\partial \mathbf{q}_k} - \frac{\dot{s}}{s} \mathbf{p}_k = \mathbf{f}_k - \frac{\dot{s}}{s} \mathbf{p}_k , \quad (12)$$

$$\dot{s} = s \frac{P_s}{Q} , \quad (13)$$

$$\dot{P}_s = \sum_{k=1}^N \frac{\mathbf{p}_k^2}{m_k} - 3Nk_B T = 3Nk_B (T(t) - T) , \quad (14)$$

where s is Nosé’s scaling parameter, Q is its mass, P_s is its conjugate momentum, and the “instantaneous temperature” $T(t)$ is defined by

$$T(t) = \frac{1}{3Nk_B} \sum_{k=1}^N \frac{\mathbf{p}_k(t)^2}{m_k} . \quad (15)$$

However, in practice, it is very difficult to obtain accurate canonical distributions of complex systems at low temperatures by conventional MC or MD simulation methods. This is because simulations at low temperatures tend to get trapped in one or a few of local-minimum-energy states.

In the multicanonical ensemble [14, 15], on the other hand, each state is weighted by a non-Boltzmann weight factor $W_{\text{mu}}(E)$ (which we refer to as the *multicanonical weight factor*) so that a uniform potential energy distribution $P_{\text{mu}}(E)$ is obtained:

$$P_{\text{mu}}(E) \propto n(E)W_{\text{mu}}(E) \equiv \text{const} . \quad (16)$$

The flat distribution implies that a free random walk in the potential energy space is realized in this ensemble. This allows the simulation to escape from any local minimum-energy states and to sample the configurational space much more widely than the conventional canonical MC or MD methods.

The definition in Eq. (16) implies that the multicanonical weight factor is inversely proportional to the density of states, and we can write it as follows:

$$W_{\text{mu}}(E) \equiv \exp[-\beta_0 E_{\text{mu}}(E; T_0)] = \frac{1}{n(E)} , \quad (17)$$

where we have chosen an arbitrary reference temperature, $T_0 = 1/k_B\beta_0$, and the “*multicanonical potential energy*” is defined by

$$E_{\text{mu}}(E; T_0) \equiv k_B T_0 \ln n(E) = T_0 S(E) . \quad (18)$$

Here, $S(E)$ is the entropy in the microcanonical ensemble. Since the density of states of the system is usually unknown, the multicanonical weight factor has to be determined numerically by iterations of short preliminary runs [14, 15].

A multicanonical MC simulation is performed, for instance, with the usual Metropolis criterion [120]: The transition probability of state x with potential energy E to state x' with potential energy E' is given by

$$w(x \rightarrow x') = \min \left(1, \frac{W_{\text{mu}}(E')}{W_{\text{mu}}(E)} \right) = \min \left(1, \frac{n(E)}{n(E')} \right) = \min (1, \exp(-\beta_0 \Delta E_{\text{mu}})) , \quad (19)$$

where

$$\Delta E_{\text{mu}} = E_{\text{mu}}(E'; T_0) - E_{\text{mu}}(E; T_0) . \quad (20)$$

The MD algorithm in the multicanonical ensemble also naturally follows from Eq. (17), in which the regular constant temperature MD simulation (with $T = T_0$) is performed by replacing E by E_{mu} in Eq. (12) [41, 44]:

$$\dot{\mathbf{p}}_k = - \frac{\partial E_{\text{mu}}(E; T_0)}{\partial \mathbf{q}_k} - \frac{\dot{s}}{s} \mathbf{p}_k = \frac{\partial E_{\text{mu}}(E; T_0)}{\partial E} \mathbf{f}_k - \frac{\dot{s}}{s} \mathbf{p}_k . \quad (21)$$

From Eq. (18) this equation can be rewritten as

$$\dot{\mathbf{p}}_k = \frac{T_0}{T(E)} \mathbf{f}_k - \frac{\dot{s}}{s} \mathbf{p}_k . \quad (22)$$

where the following thermodynamic relation gives the definition of the ‘‘effective temperature’’ $T(E)$:

$$\left. \frac{\partial S(E)}{\partial E} \right|_{E=E_a} = \frac{1}{T(E_a)} , \quad (23)$$

with

$$E_a = \langle E \rangle_{T(E_a)} . \quad (24)$$

If the exact multicanonical weight factor $W_{\text{mu}}(E)$ is known, one can calculate the ensemble averages of any physical quantity A at any temperature T ($= 1/k_B\beta$) as follows:

$$\langle A \rangle_{T=} = \frac{\sum_E A(E) P_B(E; T)}{\sum_E P_B(E; T)} = \frac{\sum_E A(E) n(E) \exp(-\beta E)}{\sum_E n(E) \exp(-\beta E)} , \quad (25)$$

where the density of states is given by (see Eq. (17))

$$n(E) = \frac{1}{W_{\text{mu}}(E)} . \quad (26)$$

The summation instead of integration is used in Eq. (25), because we often discretize the potential energy E with step size ϵ ($E = E_i; i = 1, 2, \dots$). Here, the explicit form of the physical quantity A should be known as a function of potential energy E . For instance, $A(E) = E$ gives the average potential energy $\langle E \rangle_T$ as a function of temperature, and $A(E) = \beta^2(E - \langle E \rangle_T)^2$ gives specific heat.

In general, the multicanonical weight factor $W_{\text{mu}}(E)$, or the density of states $n(E)$, is not *a priori* known, and one needs its estimator for a numerical simulation. This estimator is usually obtained from iterations of short trial multicanonical simulations. The details of this process are described, for instance, in Refs. [27, 36]. However, the iterative process can be non-trivial and very tedious for complex systems.

In practice, it is impossible to obtain the ideal multicanonical weight factor with completely uniform potential energy distribution. The question is when to stop the iteration for the weight factor determination. Our criterion for a satisfactory weight factor is that as long as we do get a random walk in potential energy space, the probability distribution $P_{\text{mu}}(E)$ does not have to be completely flat with a tolerance of, say, an order of magnitude

deviation. In such a case, we usually perform with this weight factor a multicanonical simulation with high statistics (production run) in order to get even better estimate of the density of states. Let $N_{\text{mu}}(E)$ be the histogram of potential energy distribution $P_{\text{mu}}(E)$ obtained by this production run. The best estimate of the density of states can then be given by the single-histogram reweighting techniques [8] as follows (see the proportionality relation in Eq. (16)):

$$n(E) = \frac{N_{\text{mu}}(E)}{W_{\text{mu}}(E)} . \quad (27)$$

By substituting this quantity into Eq. (25), one can calculate ensemble averages of physical quantity $A(E)$ as a function of temperature. Moreover, ensemble averages of any physical quantity A (including those that cannot be expressed as functions of potential energy) at any temperature T ($= 1/k_B\beta$) can now be obtained as long as one stores the “trajectory” of configurations (and A) from the production run. Namely, we have

$$\langle A \rangle_{T=} = \frac{\sum_{k=1}^{n_0} A(x(k)) W_{\text{mu}}^{-1}(E(x(k))) \exp[-\beta E(x(k))]}{\sum_{k=1}^{n_0} W_{\text{mu}}^{-1}(E(x(k))) \exp[-\beta E(x(k))]} , \quad (28)$$

where $x(k)$ is the configuration at the k -th MC (or MD) step and n_0 is the total number of configurations stored. Note that when A is a function of E , Eq. (28) reduces to Eq. (25) where the density of states is given by Eq. (27).

Eqs. (25) and (28) or any other equations which involve summations of exponential functions often encounter with numerical difficulties such as overflows. These can be overcome by using, for instance, the following equation [123, 124]: For $C = A + B$ (with $A > 0$ and $B > 0$) we have

$$\begin{aligned} \ln C &= \ln \left[\max(A, B) \left(1 + \frac{\min(A, B)}{\max(A, B)} \right) \right] , \\ &= \max(\ln A, \ln B) + \ln \{ 1 + \exp[\min(\ln A, \ln B) - \max(\ln A, \ln B)] \} . \end{aligned} \quad (29)$$

We now briefly review the original *simulated tempering* (ST) method [66, 67]. In this method temperature itself becomes a dynamical variable, and both the configuration and the temperature are updated during the simulation with a weight:

$$W_{\text{ST}}(E; T) = \exp(-\beta E + a(T)) , \quad (30)$$

where the function $a(T)$ is chosen so that the probability distribution of temperature is flat:

$$P_{\text{ST}}(T) = \int dE n(E) W_{\text{ST}}(E; T) = \int dE n(E) \exp(-\beta E + a(T)) = \text{const} . \quad (31)$$

Hence, in simulated tempering the *temperature* is sampled uniformly. A free random walk in temperature space is realized, which in turn induces a random walk in potential energy space and allows the simulation to escape from states of energy local minima.

In the numerical work we discretize the temperature in M different values, T_m ($m = 1, \dots, M$). Without loss of generality we can order the temperature so that $T_1 < T_2 < \dots < T_M$. The lowest temperature T_1 should be sufficiently low so that the simulation

can explore the global-minimum-energy region, and the highest temperature T_M should be sufficiently high so that no trapping in an energy-local-minimum state occurs. The probability weight factor in Eq. (30) is now written as

$$W_{\text{ST}}(E; T_m) = \exp(-\beta_m E + a_m) , \quad (32)$$

where $a_m = a(T_m)$ ($m = 1, \dots, M$). Note that from Eqs. (31) and (32) we have

$$\exp(-a_m) \propto \int dE n(E) \exp(-\beta_m E) . \quad (33)$$

The parameters a_m are therefore “dimensionless” Helmholtz free energy at temperature T_m (i.e., the inverse temperature β_m multiplied by the Helmholtz free energy). We remark that the density of states $n(E)$ (and hence, the multicanonical weight factor) and the simulated tempering weight factor a_m are related by a Laplace transform [42]. The knowledge of one implies that of the other, although in numerical work the inverse Laplace transform of Eq. (33) is nontrivial.

Once the parameters a_m are determined and the initial configuration and the initial temperature T_m are chosen, a simulated tempering simulation is then realized by alternately performing the following two steps [66, 67]:

1. A canonical MC or MD simulation at the fixed temperature T_m (based on Eq. (7) or Eq. (10)) is carried out for a certain steps.
2. The temperature T_m is updated to the neighboring values $T_{m\pm 1}$ with the configuration fixed. The transition probability of this temperature-updating process is given by the Metropolis criterion (see Eq. (32)):

$$w(T_m \rightarrow T_{m\pm 1}) = \min \left(1, \frac{W_{\text{ST}}(E; T_{m\pm 1})}{W_{\text{ST}}(E; T_m)} \right) = \min (1, \exp(-\Delta)) , \quad (34)$$

where

$$\Delta = (\beta_{m\pm 1} - \beta_m) E - (a_{m\pm 1} - a_m) . \quad (35)$$

Note that in Step 2 we exchange only pairs of neighboring temperatures in order to secure sufficiently large acceptance ratio of temperature updates.

As in multicanonical algorithm, the simulated tempering parameters $a_m = a(T_m)$ ($m = 1, \dots, M$) are also determined by iterations of short trial simulations (see, e.g., Refs. [68, 69, 43] for details). This process can be non-trivial and very tedious for complex systems.

After the optimal simulated tempering weight factor is determined, one performs a long simulated tempering run once. The canonical expectation value of a physical quantity A at temperature T_m ($m = 1, \dots, M$) can be calculated by the usual arithmetic mean as follows:

$$\langle A \rangle_{T_m} = \frac{1}{n_m} \sum_{k=1}^{n_m} A(x_m(k)) , \quad (36)$$

where $x_m(k)$ ($k = 1, \dots, n_m$) are the configurations obtained at temperature T_m and n_m is the total number of measurements made at $T = T_m$. The expectation value at any intermediate temperature can also be obtained from Eq. (25), where the density of states is given by the multiple-histogram reweighting techniques [9, 10] as follows. Let $N_m(E)$

and n_m be respectively the potential-energy histogram and the total number of samples obtained at temperature $T_m = 1/k_B\beta_m$ ($m = 1, \dots, M$). The best estimate of the density of states is then given by [9, 10]

$$n(E) = \frac{\sum_{m=1}^M g_m^{-1} N_m(E)}{\sum_{m=1}^M g_m^{-1} n_m \exp(f_m - \beta_m E)}, \quad (37)$$

where we have for each m ($= 1, \dots, M$)

$$\exp(-f_m) = \sum_E n(E) \exp(-\beta_m E). \quad (38)$$

Here, $g_m = 1 + 2\tau_m$, and τ_m is the integrated autocorrelation time at temperature T_m . For many systems the quantity g_m can safely be set to be a constant in the reweighting formulae [10], and hereafter we set $g_m = 1$.

Note that Eqs. (37) and (38) are solved self-consistently by iteration [9, 10] to obtain the density of states $n(E)$ and the dimensionless Helmholtz free energy f_m . Namely, we can set all the f_m ($m = 1, \dots, M$) to, e.g., zero initially. We then use Eq. (37) to obtain $n(E)$, which is substituted into Eq. (38) to obtain next values of f_m , and so on.

Moreover, ensemble averages of any physical quantity A (including those that cannot be expressed as functions of potential energy) at any temperature T ($= 1/k_B\beta$) can now be obtained from the “trajectory” of configurations of the production run. Namely, we first obtain f_m ($m = 1, \dots, M$) by solving Eqs. (37) and (38) self-consistently, and then we have [93]

$$\langle A \rangle_T = \frac{\sum_{m=1}^M \sum_{k=1}^{n_m} A(x_m(k)) \frac{1}{\sum_{\ell=1}^M n_\ell \exp[f_\ell - \beta_\ell E(x_m(k))]} \exp[-\beta E(x_m(k))]}{\sum_{m=1}^M \sum_{k=1}^{n_m} \frac{1}{\sum_{\ell=1}^M n_\ell \exp[f_\ell - \beta_\ell E(x_m(k))]} \exp[-\beta E(x_m(k))]}, \quad (39)$$

where $x_m(k)$ ($k = 1, \dots, n_m$) are the configurations obtained at temperature T_m .

2.2 Replica-Exchange Method

The *replica-exchange method* (REM) [75]–[77] was developed as an extension of simulated tempering [75] (thus it is also referred to as *parallel tempering* [68]) (see, e.g., Ref. [84] for a detailed description of the algorithm). The system for REM consists of M *non-interacting* copies (or, replicas) of the original system in the canonical ensemble at M different temperatures T_m ($m = 1, \dots, M$). We arrange the replicas so that there is always exactly one replica at each temperature. Then there exists a one-to-one correspondence between replicas and temperatures; the label i ($i = 1, \dots, M$) for replicas is a permutation of the label m ($m = 1, \dots, M$) for temperatures, and vice versa:

$$\begin{cases} i &= i(m) \equiv f(m), \\ m &= m(i) \equiv f^{-1}(i), \end{cases} \quad (40)$$

where $f(m)$ is a permutation function of m and $f^{-1}(i)$ is its inverse.

Let $X = \{x_1^{[i(1)]}, \dots, x_M^{[i(M)]}\} = \{x_{m(1)}^{[1]}, \dots, x_{m(M)}^{[M]}\}$ stand for a “state” in this generalized ensemble. Each “substate” $x_m^{[i]}$ is specified by the coordinates $q^{[i]}$ and momenta $p^{[i]}$ of N atoms in replica i at temperature T_m :

$$x_m^{[i]} \equiv (q^{[i]}, p^{[i]})_m . \quad (41)$$

Because the replicas are non-interacting, the weight factor for the state X in this generalized ensemble is given by the product of Boltzmann factors for each replica (or at each temperature):

$$\begin{aligned} W_{\text{REM}}(X) &= \prod_{i=1}^M \exp \left\{ -\beta_{m(i)} H(q^{[i]}, p^{[i]}) \right\} = \prod_{m=1}^M \exp \left\{ -\beta_m H(q^{[i(m)]}, p^{[i(m)]}) \right\} , \\ &= \exp \left\{ -\sum_{i=1}^M \beta_{m(i)} H(q^{[i]}, p^{[i]}) \right\} = \exp \left\{ -\sum_{m=1}^M \beta_m H(q^{[i(m)]}, p^{[i(m)]}) \right\} , \end{aligned} \quad (42)$$

where $i(m)$ and $m(i)$ are the permutation functions in Eq. (40).

We now consider exchanging a pair of replicas in the generalized ensemble. Suppose we exchange replicas i and j which are at temperatures T_m and T_n , respectively:

$$X = \{\dots, x_m^{[i]}, \dots, x_n^{[j]}, \dots\} \longrightarrow X' = \{\dots, x_m^{[j]'}, \dots, x_n^{[i]'}, \dots\} . \quad (43)$$

Here, $i, j, m,$ and n are related by the permutation functions in Eq. (40), and the exchange of replicas introduces a new permutation function f' :

$$\begin{cases} i = f(m) \longrightarrow j = f'(m) , \\ j = f(n) \longrightarrow i = f'(n) . \end{cases} \quad (44)$$

The exchange of replicas can be written in more detail as

$$\begin{cases} x_m^{[i]} \equiv (q^{[i]}, p^{[i]})_m \longrightarrow x_m^{[j]'} \equiv (q^{[j]}, p^{[j]'})_m , \\ x_n^{[j]} \equiv (q^{[j]}, p^{[j]})_n \longrightarrow x_n^{[i]'} \equiv (q^{[i]}, p^{[i]'})_n , \end{cases} \quad (45)$$

where the definitions for $p^{[i]'}$ and $p^{[j]'}$ will be given below. We remark that this process is equivalent to exchanging a pair of temperatures T_m and T_n for the corresponding replicas i and j as follows:

$$\begin{cases} x_m^{[i]} \equiv (q^{[i]}, p^{[i]})_m \longrightarrow x_n^{[i]'} \equiv (q^{[i]}, p^{[i]'})_n , \\ x_n^{[j]} \equiv (q^{[j]}, p^{[j]})_n \longrightarrow x_m^{[j]'} \equiv (q^{[j]}, p^{[j]'})_m . \end{cases} \quad (46)$$

In the original implementation of the *replica-exchange method* (REM) [75]–[77], Monte Carlo algorithm was used, and only the coordinates q (and the potential energy function $E(q)$) had to be taken into account. In molecular dynamics algorithm, on the other hand, we also have to deal with the momenta p . We proposed the following momentum assignment in Eq. (45) (and in Eq. (46)) [84]:

$$\begin{cases} p^{[i]'} \equiv \sqrt{\frac{T_n}{T_m}} p^{[i]} , \\ p^{[j]'} \equiv \sqrt{\frac{T_m}{T_n}} p^{[j]} , \end{cases} \quad (47)$$

which we believe is the simplest and the most natural. This assignment means that we just rescale uniformly the velocities of all the atoms in the replicas by the square root of the ratio of the two temperatures so that the temperature condition in Eq. (4) may be satisfied.

In order for this exchange process to converge towards an equilibrium distribution, it is sufficient to impose the detailed balance condition on the transition probability $w(X \rightarrow X')$:

$$\frac{W_{\text{REM}}(X)}{Z} w(X \rightarrow X') = \frac{W_{\text{REM}}(X')}{Z} w(X' \rightarrow X) , \quad (48)$$

where Z is the partition function of the entire system. From Eqs. (1), (2), (42), (47), and (48), we have

$$\begin{aligned} \frac{W_{\text{REM}}(X')}{W_{\text{REM}}(X)} &= \exp \left\{ -\beta_m \left[K(p^{[j]'}) + E(q^{[j]}) \right] - \beta_n \left[K(p^{[i]'}) + E(q^{[i]}) \right] \right. \\ &\quad \left. + \beta_m \left[K(p^{[i]}) + E(q^{[i]}) \right] + \beta_n \left[K(p^{[j]}) + E(q^{[j]}) \right] \right\} , \\ &= \exp \left\{ -\beta_m \frac{T_m}{T_n} K(p^{[j]}) - \beta_n \frac{T_n}{T_m} K(p^{[i]}) + \beta_m K(p^{[i]}) + \beta_n K(p^{[j]}) \right. \\ &\quad \left. - \beta_m \left[E(q^{[j]}) - E(q^{[i]}) \right] - \beta_n \left[E(q^{[i]}) - E(q^{[j]}) \right] \right\} , \\ &= \exp(-\Delta) , \end{aligned} \quad (49)$$

where

$$\Delta = \beta_m \left(E(q^{[j]}) - E(q^{[i]}) \right) - \beta_n \left(E(q^{[j]}) - E(q^{[i]}) \right) , \quad (50)$$

$$= (\beta_m - \beta_n) \left(E(q^{[j]}) - E(q^{[i]}) \right) , \quad (51)$$

and $i, j, m,$ and n are related by the permutation functions in Eq. (40) before the exchange:

$$\begin{cases} i &= f(m) , \\ j &= f(n) . \end{cases} \quad (52)$$

This can be satisfied, for instance, by the usual Metropolis criterion [120] (see also Eqs. (7), (19), and (34)):

$$w(X \rightarrow X') \equiv w \left(x_m^{[i]} \mid x_n^{[j]} \right) = \min(1, \exp(-\Delta)) , \quad (53)$$

where in the second expression (i.e., $w(x_m^{[i]} \mid x_n^{[j]})$) we explicitly wrote the pair of replicas (and temperatures) to be exchanged. Note that this is exactly the same criterion that was originally derived for Monte Carlo algorithm [75]–[77].

Without loss of generality we can again assume $T_1 < T_2 < \dots < T_M$. A simulation of the *replica-exchange method* (REM) [75]–[77] is then realized by alternately performing the following two steps:

1. Each replica in canonical ensemble of the fixed temperature is simulated *simultaneously* and *independently* for a certain MC or MD steps.
2. A pair of replicas at neighboring temperatures, say $x_m^{[i]}$ and $x_{m+1}^{[j]}$, are exchanged with the probability $w \left(x_m^{[i]} \mid x_{m+1}^{[j]} \right)$ in Eq. (53).

Note that in Step 2 we exchange only pairs of replicas corresponding to neighboring temperatures, because the acceptance ratio of the exchange process decreases exponentially with the difference of the two β 's (see Eqs. (51) and (53)). Note also that whenever a replica exchange is accepted in Step 2, the permutation functions in Eq. (40) are updated.

The REM simulation is particularly suitable for parallel computers. Because one can minimize the amount of information exchanged among nodes, it is best to assign each replica to each node (exchanging pairs of temperature values among nodes is much faster than exchanging coordinates and momenta). This means that we keep track of the permutation function $m(i; t) = f^{-1}(i; t)$ in Eq. (40) as a function of MC or MD step t during the simulation. After parallel canonical MC or MD simulations for a certain steps (Step 1), $M/2$ pairs of replicas corresponding to neighboring temperatures are simultaneously exchanged (Step 2), and the pairing is alternated between the two possible choices, i.e., $(T_1, T_2), (T_3, T_4), \dots$ and $(T_2, T_3), (T_4, T_5), \dots$.

The major advantage of REM over other generalized-ensemble methods such as multicanonical algorithm [14, 15] and simulated tempering [66, 67] lies in the fact that the weight factor is *a priori* known (see Eq. (42)), while in the latter algorithms the determination of the weight factors can be very tedious and time-consuming. A random walk in “temperature space” is realized for each replica, which in turn induces a random walk in potential energy space. This alleviates the problem of getting trapped in states of energy local minima. In REM, however, the number of required replicas increases as the system size N increases (according to \sqrt{N}) [75]. This demands a lot of computer power for complex systems.

2.3 Replica-Exchange Multicanonical Algorithm and Replica-Exchange Simulated Tempering

The *replica-exchange multicanonical algorithm* (REMUCA) [88, 93, 94] overcomes both the difficulties of MUCA (the multicanonical weight factor determination is non-trivial) and REM (a lot of replicas, or computation time, is required). In REMUCA we first perform a short REM simulation (with M replicas) to determine the multicanonical weight factor and then perform with this weight factor a regular multicanonical simulation with high statistics. The first step is accomplished by the multiple-histogram reweighting techniques [9, 10]. Let $N_m(E)$ and n_m be respectively the potential-energy histogram and the total number of samples obtained at temperature $T_m (= 1/k_B\beta_m)$ of the REM run. The density of states $n(E)$ is then given by solving Eqs. (37) and (38) self-consistently by iteration.

Once the estimate of the density of states is obtained, the multicanonical weight factor can be directly determined from Eq. (17) (see also Eq. (18)). Actually, the density of states $n(E)$ and the multicanonical potential energy, $E_{\text{mu}}(E; T_0)$, thus determined are only reliable in the following range:

$$E_1 \leq E \leq E_M , \quad (54)$$

where

$$\begin{cases} E_1 &= \langle E \rangle_{T_1} , \\ E_M &= \langle E \rangle_{T_M} , \end{cases} \quad (55)$$

and T_1 and T_M are respectively the lowest and the highest temperatures used in the REM run. Outside this range we extrapolate the multicanonical potential energy linearly: [88]

$$\mathcal{E}_{\text{mu}}^{\{0\}}(E) \equiv \begin{cases} \left. \frac{\partial E_{\text{mu}}(E; T_0)}{\partial E} \right|_{E=E_1} (E - E_1) + E_{\text{mu}}(E_1; T_0) , & \text{for } E < E_1, \\ E_{\text{mu}}(E; T_0) , & \text{for } E_1 \leq E \leq E_M, \\ \left. \frac{\partial E_{\text{mu}}(E; T_0)}{\partial E} \right|_{E=E_M} (E - E_M) + E_{\text{mu}}(E_M; T_0) , & \text{for } E > E_M. \end{cases} \quad (56)$$

The multicanonical MC and MD runs are then performed respectively with the Metropolis criterion of Eq. (19) and with the modified Newton equation in Eq. (21), in which $\mathcal{E}_{\text{mu}}^{\{0\}}(E)$ in Eq. (56) is substituted into $E_{\text{mu}}(E; T_0)$. We expect to obtain a flat potential energy distribution in the range of Eq. (54). Finally, the results are analyzed by the single-histogram reweighting techniques as described in Eq. (27) (and Eq. (25)).

Some remarks are now in order. From Eqs. (18), (23), (24), and (55), Eq. (56) becomes

$$\mathcal{E}_{\text{mu}}^{\{0\}}(E) = \begin{cases} \frac{T_0}{T_1}(E - E_1) + T_0 S(E_1) = \frac{T_0}{T_1}E + \text{const} , & \text{for } E < E_1 \equiv \langle E \rangle_{T_1}, \\ T_0 S(E) , & \text{for } E_1 \leq E \leq E_M, \\ \frac{T_0}{T_M}(E - E_M) + T_0 S(E_M) = \frac{T_0}{T_M}E + \text{const} , & \text{for } E > E_M \equiv \langle E \rangle_{T_M}. \end{cases} \quad (57)$$

The Newton equation in Eq. (21) is then written as (see Eqs. (22), (23), and (24))

$$\dot{\mathbf{p}}_k = \begin{cases} \frac{T_0}{T_1} \mathbf{f}_k - \frac{\dot{s}}{s} \mathbf{p}_k , & \text{for } E < E_1, \\ \frac{T_0}{T(E)} \mathbf{f}_k - \frac{\dot{s}}{s} \mathbf{p}_k , & \text{for } E_1 \leq E \leq E_M, \\ \frac{T_0}{T_M} \mathbf{f}_k - \frac{\dot{s}}{s} \mathbf{p}_k , & \text{for } E > E_M. \end{cases} \quad (58)$$

Because only the product of inverse temperature β and potential energy E enters in the Boltzmann factor (see Eq. (5)), a rescaling of the potential energy (or force) by a constant, say α , can be considered as the rescaling of the temperature by $1/\alpha$ [41, 101]. Hence, our choice of $\mathcal{E}_{\text{mu}}^{\{0\}}(E)$ in Eq. (56) results in a canonical simulation at $T = T_1$ for $E < E_1$, a multicanonical simulation for $E_1 \leq E \leq E_M$, and a canonical simulation at $T = T_M$ for $E > E_M$. Note also that the above arguments are independent of the value of T_0 , and we will get the same results, regardless of its value.

For Monte Carlo method, the above statement follows directly from the following equation. Namely, our choice of the multicanonical potential energy in Eq. (56) gives (by substituting Eq. (57) into Eq. (17))

$$W_{\text{mu}}(E) = \exp \left[-\beta_0 \mathcal{E}_{\text{mu}}^{\{0\}}(E) \right] = \begin{cases} \exp(-\beta_1 E + \text{const}) , & \text{for } E < E_1, \\ \frac{1}{n(E)} , & \text{for } E_1 \leq E \leq E_M, \\ \exp(-\beta_M E + \text{const}) , & \text{for } E > E_M. \end{cases} \quad (59)$$

We now present another effective method of the multicanonical weight factor determination [3], which is closely related to REMUCA. We first perform a short REM simulation as in REMUCA and calculate $\langle E \rangle_T$ as a function of T by the multiple-histogram

reweighting techniques (see Eqs. (37) and (38)). Let us recall the Newton equation of Eq. (22) and the thermodynamic relation of Eqs. (23) and (24). The effective temperature $T(E)$, or the derivative $\frac{\partial E_{\text{mu}}(E; T_0)}{\partial E}$, can be numerically obtained as the inverse function of Eq. (24), where the average $\langle E \rangle_{T(E)}$ has been obtained from the results of the REM simulation by the multiple-histogram reweighting techniques. Given its derivative, the multicanonical potential energy can then be obtained by numerical integration (see Eqs. (18) and (23)): [3]

$$E_{\text{mu}}(E; T_0) = T_0 \int_{E_1}^E \frac{\partial S(E)}{\partial E} dE = T_0 \int_{E_1}^E \frac{dE}{T(E)}. \quad (60)$$

We remark that the same equation was used to obtain the multicanonical weight factor in Ref. [72], where $\langle E \rangle_T$ was estimated by simulated annealing instead of REM. Essentially the same formulation was also recently used in Ref. [61] to obtain the multicanonical potential energy, where $\langle E \rangle_T$ was calculated by conventional canonical simulations.

We finally present the new method which we refer to as the *replica-exchange simulated tempering* (REST) [89]. In this method, just as in REMUCA, we first perform a short REM simulation (with M replicas) to determine the simulated tempering weight factor and then perform with this weight factor a regular ST simulation with high statistics. The first step is accomplished by the multiple-histogram reweighting techniques [9, 10], which give the dimensionless Helmholtz free energy f_m (see Eqs. (37) and (38)).

Once the estimate of the dimensionless Helmholtz free energy f_m are obtained, the simulated tempering weight factor can be directly determined by using Eq. (32) where we set $a_m = f_m$ (compare Eq. (33) with Eq. (38)). A long simulated tempering run is then performed with this weight factor. Let $N_m(E)$ and n_m be respectively the potential-energy histogram and the total number of samples obtained at temperature $T_m (= 1/k_B\beta_m)$ from this simulated tempering run. The multiple-histogram reweighting techniques of Eqs. (37) and (38) can be used again to obtain the best estimate of the density of states $n(E)$. The expectation value of a physical quantity A at any temperature $T (= 1/k_B\beta)$ is then calculated from Eq. (25).

The formulations of REMUCA and REST are simple and straightforward, but the numerical improvement is great, because the weight factor determination for MUCA and ST becomes very difficult by the usual iterative processes for complex systems.

2.4 Multicanonical Replica-Exchange Method and Simulated Tempering Replica-Exchange Method

In the previous subsection we presented REMUCA, which uses a short REM run for the determination of the multicanonical weight factor. Here, we present two modifications of REM and refer the new methods as multicanonical replica-exchange method (MUCAREM) [88, 93, 94] and simulated tempering replica-exchange method (STREM) [115]. In MUCAREM the production run is a REM simulation with a few replicas not in the canonical ensemble but in the multicanonical ensemble, i.e., different replicas perform MUCA simulations with different energy ranges. Likewise in STREM the production run is a REM simulation with a few replicas that performs ST simulations with different temperature ranges. While MUCA and ST simulations are usually based on local updates, a replica-exchange process can be considered to be a global update, and global updates enhance the sampling further.

We first describe MUCAREM. Let \mathcal{M} be the number of replicas. Here, each replica is in one-to-one correspondence not with temperature but with multicanonical weight factors of different energy range. Note that because multicanonical simulations cover much wider energy ranges than regular canonical simulations, the number of required replicas for the production run of MUCAREM is much less than that for the regular REM ($\mathcal{M} \ll M$). The weight factor for this generalized ensemble is now given by (see Eq. (42))

$$W_{\text{MUCAREM}}(X) = \prod_{i=1}^{\mathcal{M}} W_{\text{mu}}^{\{m(i)\}} \left(E \left(x_{m(i)}^{[i]} \right) \right) = \prod_{m=1}^{\mathcal{M}} W_{\text{mu}}^{\{m\}} \left(E \left(x_m^{[i(m)]} \right) \right), \quad (61)$$

where we prepare the multicanonical weight factor (and the density of states) separately for m regions (see Eq. (17)):

$$W_{\text{mu}}^{\{m\}} \left(E \left(x_m^{[i]} \right) \right) = \exp \left[-\beta_m \mathcal{E}_{\text{mu}}^{\{m\}} \left(E \left(x_m^{[i]} \right) \right) \right] \equiv \frac{1}{n^{\{m\}} \left(E \left(x_m^{[i]} \right) \right)}. \quad (62)$$

Here, we have introduced \mathcal{M} arbitrary reference temperatures $T_m = 1/k_B \beta_m$ ($m = 1, \dots, \mathcal{M}$), but the final results will be independent of the values of T_m , as one can see from the second equality in Eq. (62) (these arbitrary temperatures are necessary only for MD simulations).

Each multicanonical weight factor $W_{\text{mu}}^{\{m\}}(E)$, or the density of states $n^{\{m\}}(E)$, is defined as follows. For each m ($m = 1, \dots, \mathcal{M}$), we assign a pair of temperatures ($T_L^{\{m\}}, T_H^{\{m\}}$). Here, we assume that $T_L^{\{m\}} < T_H^{\{m\}}$ and arrange the temperatures so that the neighboring regions covered by the pairs have sufficient overlaps. Without loss of generality we can assume $T_L^{\{1\}} < \dots < T_L^{\{\mathcal{M}\}}$ and $T_H^{\{1\}} < \dots < T_H^{\{\mathcal{M}\}}$. We define the following quantities:

$$\begin{cases} E_L^{\{m\}} &= \langle E \rangle_{T_L^{\{m\}}} \quad , \\ E_H^{\{m\}} &= \langle E \rangle_{T_H^{\{m\}}} \quad , \end{cases} \quad (m = 1, \dots, \mathcal{M}). \quad (63)$$

Suppose that the multicanonical weight factor $W_{\text{mu}}(E)$ (or equivalently, the multicanonical potential energy $E_{\text{mu}}(E; T_0)$ in Eq. (18)) has been obtained as in REMUCA or by any other methods in the entire energy range of interest ($E_L^{\{1\}} < E < E_H^{\{\mathcal{M}\}}$). We then have for each m ($m = 1, \dots, \mathcal{M}$) the following multicanonical potential energies (see Eq. (56)): [88]

$$\mathcal{E}_{\text{mu}}^{\{m\}}(E) = \begin{cases} \frac{\partial E_{\text{mu}}(E_L^{\{m\}}; T_m)}{\partial E} (E - E_L^{\{m\}}) + E_{\text{mu}}(E_L^{\{m\}}; T_m) \quad , & \text{for } E < E_L^{\{m\}}, \\ E_{\text{mu}}(E; T_m) \quad , & \text{for } E_L^{\{m\}} \leq E \leq E_H^{\{m\}}, \\ \frac{\partial E_{\text{mu}}(E_H^{\{m\}}; T_m)}{\partial E} (E - E_H^{\{m\}}) + E_{\text{mu}}(E_H^{\{m\}}; T_m) \quad , & \text{for } E > E_H^{\{m\}}. \end{cases} \quad (64)$$

Finally, a MUCAREM simulation is realized by alternately performing the following two steps.

1. Each replica of the fixed multicanonical ensemble is simulated *simultaneously* and *independently* for a certain MC or MD steps.

2. A pair of replicas, say i and j , which are in neighboring multicanonical ensembles, say m -th and $(m+1)$ -th, respectively, are exchanged: $X = \{\dots, x_m^{[i]}, \dots, x_{m+1}^{[j]}, \dots\} \rightarrow X' = \{\dots, x_m^{[j]}, \dots, x_{m+1}^{[i]}, \dots\}$. The transition probability of this replica exchange is given by the Metropolis criterion:

$$w(X \rightarrow X') = \min(1, \exp(-\Delta)) , \quad (65)$$

where we now have (see Eq. (50)) [88]

$$\begin{aligned} \Delta &= \beta_m \left\{ \mathcal{E}_{\text{mu}}^{\{m\}}(E(q^{[j]})) - \mathcal{E}_{\text{mu}}^{\{m\}}(E(q^{[i]})) \right\} \\ &\quad - \beta_{m+1} \left\{ \mathcal{E}_{\text{mu}}^{\{m+1\}}(E(q^{[j]})) - \mathcal{E}_{\text{mu}}^{\{m+1\}}(E(q^{[i]})) \right\} . \end{aligned} \quad (66)$$

Here, $E(q^{[i]})$ and $E(q^{[j]})$ are the potential energy of the i -th replica and the j -th replica, respectively.

Note that in Eq. (66) we need to newly evaluate the multicanonical potential energy, $\mathcal{E}_{\text{mu}}^{\{m\}}(E(q^{[j]}))$ and $\mathcal{E}_{\text{mu}}^{\{m+1\}}(E(q^{[i]}))$, because $\mathcal{E}_{\text{mu}}^{\{m\}}(E)$ and $\mathcal{E}_{\text{mu}}^{\{n\}}(E)$ are, in general, different functions for $m \neq n$.

In this algorithm, the m -th multicanonical ensemble actually results in a canonical simulation at $T = T_L^{\{m\}}$ for $E < E_L^{\{m\}}$, a multicanonical simulation for $E_L^{\{m\}} \leq E \leq E_H^{\{m\}}$, and a canonical simulation at $T = T_H^{\{m\}}$ for $E > E_H^{\{m\}}$, while the replica-exchange process samples states of the whole energy range ($E_L^{\{1\}} \leq E \leq E_H^{\{\mathcal{M}\}}$).

For obtaining the canonical distributions at any intermediate temperature T , the multiple-histogram reweighting techniques [9, 10] are again used. Let $N_m(E)$ and n_m be respectively the potential-energy histogram and the total number of samples obtained with the multicanonical weight factor $W_{\text{mu}}^{\{m\}}(E)$ ($m = 1, \dots, \mathcal{M}$). The expectation value of a physical quantity A at any temperature T ($= 1/k_B\beta$) is then obtained from Eq. (25), where the best estimate of the density of states is obtained by solving the WHAM equations, which now read [88]

$$n(E) = \frac{\sum_{m=1}^{\mathcal{M}} N_m(E)}{\sum_{m=1}^{\mathcal{M}} n_m \exp(f_m) W_{\text{mu}}^{\{m\}}(E)} = \frac{\sum_{m=1}^{\mathcal{M}} N_m(E)}{\sum_{m=1}^{\mathcal{M}} n_m \exp(f_m - \beta_m \mathcal{E}_{\text{mu}}^{\{m\}}(E))} , \quad (67)$$

and for each m ($= 1, \dots, \mathcal{M}$)

$$\exp(-f_m) = \sum_E n(E) W_{\text{mu}}^{\{m\}}(E) = \sum_E n(E) \exp(-\beta_m \mathcal{E}_{\text{mu}}^{\{m\}}(E)) . \quad (68)$$

Note that $W_{\text{mu}}^{\{m\}}(E)$ is used instead of the Boltzmann factor $\exp(-\beta_m E)$ in Eqs. (37) and (38).

Moreover, ensemble averages of any physical quantity A (including those that cannot be expressed as functions of potential energy) at any temperature T ($= 1/k_B\beta$) can now be obtained from the “trajectory” of configurations of the production run. Namely, we first obtain f_m ($m = 1, \dots, \mathcal{M}$) by solving Eqs. (67) and (68) self-consistently, and then

we have [93]

$$\langle A \rangle_T = \frac{\sum_{m=1}^{\mathcal{M}} \sum_{k=1}^{n_m} A(x_m(k)) \frac{1}{\sum_{\ell=1}^{\mathcal{M}} n_\ell \exp(f_\ell) W_{\text{mu}}^{\{\ell\}}(E(x_m(k)))} \exp[-\beta E(x_m(k))]}{\sum_{m=1}^{\mathcal{M}} \sum_{k=1}^{n_m} \frac{1}{\sum_{\ell=1}^{\mathcal{M}} n_\ell \exp(f_\ell) W_{\text{mu}}^{\{\ell\}}(E(x_m(k)))} \exp[-\beta E(x_m(k))]}, \quad (69)$$

where the trajectories $x_m(k)$ ($k = 1, \dots, n_m$) are taken from each multicanonical simulation with the multicanonical weight factor $W_{\text{mu}}^{\{m\}}(E)$ ($m = 1, \dots, \mathcal{M}$) separately. are

As seen above, both REMUCA and MUCAREM can be used to obtain the multicanonical weight factor, or the density of states, for the entire potential energy range of interest. For complex systems, however, a single REMUCA or MUCAREM simulation is often insufficient. In such cases we can iterate MUCA (in REMUCA) and/or MUCAREM simulations in which the estimate of the multicanonical weight factor is updated by the single- and/or multiple-histogram reweighting techniques, respectively.

To be more specific, this iterative process can be summarized as follows. The REMUCA production run corresponds to a MUCA simulation with the weight factor $W_{\text{mu}}(E)$. The new estimate of the density of states can be obtained by the single-histogram reweighting techniques of Eq. (27). On the other hand, from the MUCAREM production run, the improved density of states can be obtained by the multiple-histogram reweighting techniques of Eqs. (67) and (68).

The improved density of states thus obtained leads to a new multicanonical weight factor (see Eq. (17)). The next iteration can be either a MUCA production run (as in REMUCA) or MUCAREM production run. The results of this production run may yield an optimal multicanonical weight factor that yields a sufficiently flat energy distribution for the entire energy range of interest. If not, we can repeat the above process by obtaining the third estimate of the multicanonical weight factor either by a MUCA production run (as in REMUCA) or by a MUCAREM production run, and so on.

We remark that as the estimate of the multicanonical weight factor becomes more accurate, one is required to have a less number of replicas for a successful MUCAREM simulation, because each replica will have a flat energy distribution for a wider energy range. Hence, for a large, complex system, it is often more efficient to first try MUCAREM and iteratively reduce the number of replicas so that eventually one needs only one or a few replicas (instead of trying REMUCA directly from the beginning and iterating MUCA simulations).

We now describe the simulated tempering replica-exchange method (STREM) [115]. Suppose that the simulated tempering weight factor $W_{ST}(E; T_n)$ (or equivalently, the dimensionless Helmholtz free energy a_n in Eq. (32)) has been obtained as in REST or by any other methods in the entire temperature range of interest ($T_1 \leq T_n \leq T_M$). We divide the overlapping temperature ranges into \mathcal{M} regions ($\mathcal{M} \ll M$). Suppose each temperature range m has \mathcal{N}_m temperatures: $T_k^{\{m\}}$ ($k = 1, \dots, \mathcal{N}_m$) for $m = 1, \dots, \mathcal{M}$. We assign each temperature range to a replica; each replica i is in one-to-one correspondence with

a different temperature range m of ST run, where $T_1^{\{m\}} \leq T_k^{\{m\}} \leq T_{\mathcal{N}_m}^{\{m\}}$ ($k = 1, \dots, \mathcal{N}_m$). We then introduce the replica-exchange process between neighboring temperature ranges. This works when we allow sufficient overlaps between the temperature regions.

A STREM simulation is then realized by alternately performing the following two steps. [115]

1. Each replica performs a ST simulation within the fixed temperature range *simultaneously* and *independently* for a certain MC or MD steps.
2. A pair of replicas, say i and j , which are at, say $T = T_k^{\{m\}}$ and $T = T_\ell^{\{m+1\}}$, in neighboring temperature ranges, say m -th and $(m + 1)$ -th, respectively, are exchanged: $X = \{\dots, x_k^{[i]}, \dots, x_\ell^{[j]}, \dots\} \longrightarrow X' = \{\dots, x_k^{[j]}, \dots, x_\ell^{[i]}, \dots\}$. The transition probability of this replica exchange is given by the Metropolis criterion:

$$w(X \rightarrow X') = \min(1, \exp(-\Delta)) , \quad (70)$$

where

$$\Delta \equiv (\beta_k^{\{m\}} - \beta_\ell^{\{m+1\}}) (E(q^{[j]}) - E(q^{[i]})) . \quad (71)$$

While in MUCAREM each replica performs a random walk in multicanonical ensemble of finite energy range, in STREM each replica performs a random walk by simulated tempering of finite temperature range. These “local” random walks are made “global” to cover the entire energy range of interest by the replica-exchange process.

2.5 Multidimensional Replica-Exchange Method

We now present our multidimensional extension of REM, which we refer to as *multidimensional replica-exchange method* (MREM) [86]. The crucial observation that led to the new algorithm is: As long as we have M *non-interacting* replicas of the original system, the Hamiltonian $H(q, p)$ of the system does not have to be identical among the replicas and it can depend on a parameter with different parameter values for different replicas. Namely, we can write the Hamiltonian for the i -th replica at temperature T_m as

$$H_m(q^{[i]}, p^{[i]}) = K(p^{[i]}) + E_{\lambda_m}(q^{[i]}) , \quad (72)$$

where the potential energy E_{λ_m} depends on a parameter λ_m and can be written as

$$E_{\lambda_m}(q^{[i]}) = E_0(q^{[i]}) + \lambda_m V(q^{[i]}) . \quad (73)$$

This expression for the potential energy is often used in simulations. For instance, in umbrella sampling [21], $E_0(q)$ and $V(q)$ can be respectively taken as the original potential energy and the “biasing” potential energy with the coupling parameter λ_m . In simulations of spin systems, on the other hand, $E_0(q)$ and $V(q)$ (here, q stands for spins) can be respectively considered as the zero-field term and the magnetization term coupled with the external field λ_m .

While replica i and temperature T_m are in one-to-one correspondence in the original REM, replica i and “parameter set” $\Lambda_m \equiv (T_m, \lambda_m)$ are in one-to-one correspondence in the new algorithm. Hence, the present algorithm can be considered as a multidimensional extension of the original replica-exchange method where the “parameter space” is

one-dimensional (i.e., $\Lambda_m = T_m$). Because the replicas are non-interacting, the weight factor for the state X in this new generalized ensemble is again given by the product of Boltzmann factors for each replica (see Eq. (42)):

$$\begin{aligned} W_{\text{MREM}}(X) &= \exp \left\{ - \sum_{i=1}^M \beta_{m(i)} H_{m(i)} \left(q^{[i]}, p^{[i]} \right) \right\} , \\ &= \exp \left\{ - \sum_{m=1}^M \beta_m H_m \left(q^{[i(m)]}, p^{[i(m)]} \right) \right\} , \end{aligned} \quad (74)$$

where $i(m)$ and $m(i)$ are the permutation functions in Eq. (40). Then the same derivation that led to the original replica-exchange criterion follows, and the transition probability of replica exchange is given by Eq. (53), where we now have (see Eq. (50)) [86]

$$\Delta = \beta_m \left(E_{\lambda_m} \left(q^{[j]} \right) - E_{\lambda_m} \left(q^{[i]} \right) \right) - \beta_n \left(E_{\lambda_n} \left(q^{[j]} \right) - E_{\lambda_n} \left(q^{[i]} \right) \right) . \quad (75)$$

Here, E_{λ_m} and E_{λ_n} are the total potential energies (see Eq. (73)). Note that we need to newly evaluate the potential energy for exchanged coordinates, $E_{\lambda_m}(q^{[j]})$ and $E_{\lambda_n}(q^{[i]})$, because E_{λ_m} and E_{λ_n} are in general different functions.

For obtaining the canonical distributions, the multiple-histogram reweighting techniques [9, 10] are particularly suitable. Suppose we have made a single run of the present replica-exchange simulation with M replicas that correspond to M different parameter sets $\Lambda_m \equiv (T_m, \lambda_m)$ ($m = 1, \dots, M$). Let $N_m(E_0, V)$ and n_m be respectively the potential-energy histogram and the total number of samples obtained for the m -th parameter set Λ_m . The WHAM equations that yield the canonical probability distribution $P_{T,\lambda}(E_0, V) = n(E_0, V) \exp(-\beta E_\lambda)$ with any potential-energy parameter value λ at any temperature $T = 1/k_B\beta$ are then given by [86]

$$n(E_0, V) = \frac{\sum_{m=1}^M N_m(E_0, V)}{\sum_{m=1}^M n_m \exp(f_m - \beta_m E_{\lambda_m})} , \quad (76)$$

and for each m ($= 1, \dots, M$)

$$\exp(-f_m) = \sum_{E_0, V} n(E_0, V) \exp(-\beta_m E_{\lambda_m}) . \quad (77)$$

Here, $n(E_0, V)$ is the generalized density of states. Note that $n(E_0, V)$ is independent of the parameter sets $\Lambda_m \equiv (T_m, \lambda_m)$ ($m = 1, \dots, M$). The density of states $n(E_0, V)$ and the “dimensionless” Helmholtz free energy f_m in Eqs. (76) and (77) are solved self-consistently by iteration.

We can use MREM for free energy calculations. We first describe the free-energy perturbation case. The potential energy is given by

$$E_\lambda(q) = E_I(q) + \lambda (E_F(q) - E_I(q)) , \quad (78)$$

where E_I and E_F are the potential energy for a “wild-type” molecule and a “mutated” molecule, respectively. Note that this equation has the same form as Eq. (73).

Our replica-exchange simulation is performed for M replicas with M different values of the parameters $\Lambda_m = (T_m, \lambda_m)$. Since $E_{\lambda=0}(q) = E_I(q)$ and $E_{\lambda=1}(q) = E_F(q)$, we should choose enough λ_m values distributed in the range between 0 and 1 so that we may have sufficient acceptance of replica exchange. From the simulation, M histograms $N_m(E_I, E_F - E_I)$, or equivalently $N_m(E_I, E_F)$, are obtained. The Helmholtz free energy difference of “mutation” at temperature T ($= 1/k_B\beta$), $\Delta F \equiv F_{\lambda=1} - F_{\lambda=0}$, can then be calculated from

$$\exp(-\beta\Delta F) = \frac{Z_{T,\lambda=1}}{Z_{T,\lambda=0}} = \frac{\sum_{E_I, E_F} P_{T,\lambda=1}(E_I, E_F)}{\sum_{E_I, E_F} P_{T,\lambda=0}(E_I, E_F)}, \quad (79)$$

where $P_{T,\lambda}(E_I, E_F) = n(E_I, E_F) \exp(-\beta E_\lambda)$ are obtained from the WHAM equations of Eqs. (76) and (77).

We now describe another free energy calculations based on MREM applied to umbrella sampling [21], which we refer to as *replica-exchange umbrella sampling* (REUS). The potential energy is a generalization of Eq. (73) and is given by

$$E_{\boldsymbol{\lambda}}(q) = E_0(q) + \sum_{\ell=1}^L \lambda^{(\ell)} V_\ell(q), \quad (80)$$

where $E_0(q)$ is the original unbiased potential, $V_\ell(q)$ ($\ell = 1, \dots, L$) are the biasing (umbrella) potentials, and $\lambda^{(\ell)}$ are the corresponding coupling constants ($\boldsymbol{\lambda} = (\lambda^{(1)}, \dots, \lambda^{(L)})$). Introducing a “reaction coordinate” ξ , the umbrella potentials are usually written as harmonic restraints:

$$V_\ell(q) = k_\ell (\xi(q) - d_\ell)^2, \quad (\ell = 1, \dots, L), \quad (81)$$

where d_ℓ are the midpoints and k_ℓ are the strengths of the restraining potentials. We prepare M replicas with M different values of the parameters $\Lambda_m = (T_m, \boldsymbol{\lambda}_m)$, and the replica-exchange simulation is performed. Since the umbrella potentials $V_\ell(q)$ in Eq. (81) are all functions of the reaction coordinate ξ only, we can take the histogram $N_m(E_0, \xi)$ instead of $N_m(E_0, V_1, \dots, V_L)$. The WHAM equations of Eqs. (76) and (77) can then be written as [86]

$$n(E_0, \xi) = \frac{\sum_{m=1}^M N_m(E_0, \xi)}{\sum_{m=1}^M n_m \exp(f_m - \beta_m E_{\boldsymbol{\lambda}_m})} \quad (82)$$

and for each m ($= 1, \dots, M$)

$$\exp(-f_m) = \sum_{E_0, \xi} n(E_0, \xi) \exp(-\beta_m E_{\boldsymbol{\lambda}_m}). \quad (83)$$

The expectation value of a physical quantity A with any potential-energy parameter value $\boldsymbol{\lambda}$ at any temperature T ($= 1/k_B\beta$) is now given by

$$\langle A \rangle_{T, \boldsymbol{\lambda}} = \frac{\sum_{E_0, \xi} A(E_0, \xi) P_{T, \boldsymbol{\lambda}}(E_0, \xi)}{\sum_{E_0, \xi} P_{T, \boldsymbol{\lambda}}(E_0, \xi)}, \quad (84)$$

where $P_{T,\boldsymbol{\lambda}}(E_0, \xi) = n(E_0, \xi) \exp(-\beta E_{\boldsymbol{\lambda}})$ is obtained from the WHAM equations of Eqs. (82) and (83).

The potential of mean force (PMF), or free energy as a function of the reaction coordinate, of the original, unbiased system at temperature T is given by

$$\mathcal{W}_{T,\boldsymbol{\lambda}=\{0\}}(\xi) = -k_B T \ln \left[\sum_{E_0} P_{T,\boldsymbol{\lambda}=\{0\}}(E_0, \xi) \right], \quad (85)$$

where $\{0\} = (0, \dots, 0)$.

We now present two examples of realization of REUS. In the first example, we use only one temperature, T , and L umbrella potentials. We prepare replicas so that the potential energy for each replica includes exactly one umbrella potential (here, we have $M = L$). Namely, in Eq. (80) for $\boldsymbol{\lambda} = \boldsymbol{\lambda}_m$ we set

$$\lambda_m^{(\ell)} = \delta_{\ell,m}, \quad (86)$$

where $\delta_{k,l}$ is Kronecker's delta function, and we have

$$E_{\boldsymbol{\lambda}_m}(q^{[i]}) = E_0(q^{[i]}) + V_m(q^{[i]}). \quad (87)$$

We exchange replicas corresponding to ‘‘neighboring’’ umbrella potentials, V_m and V_{m+1} . The acceptance criterion for replica exchange is given by Eq. (53), where Eq. (75) now reads (with the fixed inverse temperature $\beta = 1/k_B T$) [86]

$$\Delta = \beta \left(V_m(q^{[j]}) - V_m(q^{[i]}) - V_{m+1}(q^{[j]}) + V_{m+1}(q^{[i]}) \right), \quad (88)$$

where replicas i and j respectively have umbrella potentials V_m and V_{m+1} before the exchange.

In the second example, we prepare N_T temperatures and L umbrella potentials, which makes the total number of replicas $M = N_T \times L$. We can introduce the following re-labeling for the parameters that characterize the replicas:

$$\begin{aligned} \boldsymbol{\Lambda}_m = (T_m, \boldsymbol{\lambda}_m) &\longrightarrow \boldsymbol{\Lambda}_{I,J} = (T_I, \boldsymbol{\lambda}_J) \\ (m = 1, \dots, M) &\quad (I = 1, \dots, N_T, J = 1, \dots, L) \end{aligned} \quad (89)$$

The potential energy is given by Eq. (87) with the replacement: $m \rightarrow J$. We perform the following replica-exchange processes alternately:

1. Exchange pairs of replicas corresponding to neighboring temperatures, T_I and T_{I+1} (i.e., exchange replicas i and j that respectively correspond to parameters $\boldsymbol{\Lambda}_{I,J}$ and $\boldsymbol{\Lambda}_{I+1,J}$). (We refer to this process as T -exchange.)
2. Exchange pairs of replicas corresponding to ‘‘neighboring’’ umbrella potentials, V_J and V_{J+1} (i.e., exchange replicas i and j that respectively correspond to parameters $\boldsymbol{\Lambda}_{I,J}$ and $\boldsymbol{\Lambda}_{I,J+1}$). (We refer to this process as λ -exchange.)

The acceptance criterion for these replica exchanges is given by Eq. (53), where Eq. (75) now reads [86]

$$\Delta = (\beta_I - \beta_{I+1}) \left(E_0(q^{[j]}) + V_J(q^{[j]}) - E_0(q^{[i]}) - V_J(q^{[i]}) \right), \quad (90)$$

for T -exchange, and

$$\Delta = \beta_I \left(V_J(q^{[j]}) - V_J(q^{[i]}) - V_{J+1}(q^{[j]}) + V_{J+1}(q^{[i]}) \right), \quad (91)$$

for λ -exchange. By this procedure, the random walk in the reaction coordinate space as well as in the temperature space can be realized.

2.6 From Multidimensional REM to Multidimensional MUCA and ST

The formulations of MREM give multidimensional/multivariable extensions of REMUCA and REST [5]. In REMUCA and in REST, the multicanonical weight factor and the simulated tempering weight factor are determined from the results of a short REM simulation, respectively. The results of a short MREM simulation can therefore be used to determine the weight factors for multidimensional/multivariable MUCA and ST simulatoins, where random walks in multidimensional “energy” and “parameter” space are realized [5]. Here, we give more details.

We consider a simple example with the following potential energy:

$$E_\lambda(q) = E_0(q) + \lambda V(q) . \quad (92)$$

In the two-dimensional multicanonical ensemble each state is weighted by the multicanonical weight factor $W_{\text{mu}}(E_0, V)$ so that a uniform potential energy distribution both in E_0 and V may be obtained:

$$P_{\text{mu}}(E_0, V) \propto n(E_0, V)W_{\text{mu}}(E_0, V) \equiv \text{const} , \quad (93)$$

where $n(E_0, V)$ is the two-dimensional density of states. This implies that

$$W_{\text{mu}}(E_0, V) \equiv \exp[-\beta_0 E_{\text{mu}}(E_0, V; T_0)] = \frac{1}{n(E_0, V)} , \quad (94)$$

where we have chosen an arbitrary reference temperature, $T_0 = 1/k_B\beta_0$, and the “*multicanonical potential energy*” is defined by

$$E_{\text{mu}}(E_0, V; T_0) \equiv k_B T_0 \ln n(E_0, V) . \quad (95)$$

The two-dimensional MUCA MC simulation can be performed with the following transition probability from state x with potential energy $E_0 + \lambda V$ to state x' with potential energy $E_0' + \lambda V'$ (see Eq. (19)):

$$w(x \rightarrow x') = \min \left(1, \frac{W_{\text{mu}}(E_0', V')}{W_{\text{mu}}(E_0, V)} \right) = \min \left(1, \frac{n(E_0, V)}{n(E_0', V')} \right) . \quad (96)$$

The MD algorithm in the two-dimensional multicanonical ensemble also naturally follows from Eq. (17), in which the regular constant temperature MD simulation (with $T = T_0$) is performed by replacing E by E_{mu} in Eq. (12) (see Eq. (21)):

$$\dot{\mathbf{p}}_k = - \frac{\partial E_{\text{mu}}(E_0, V; T_0)}{\partial \mathbf{q}_k} - \frac{\dot{s}}{s} \mathbf{p}_k . \quad (97)$$

In the two-dimensional simulated tempering, the parameter set (T, λ) become dynamical variables, and both the configuration and the parameter set are updated during the simulation with a weight (see Eq. (30)):

$$W_{\text{ST}}(E_\lambda; T, \lambda) = \exp(-\beta E_\lambda + f(T, \lambda)) , \quad (98)$$

where the function $f(T, \lambda)$ is chosen so that the probability distribution of the two-dimensional parameter set is flat (see Eq. (31)):

$$\begin{aligned} P_{\text{ST}}(T, \lambda) &= \int dE_0 dV n(E_0, V) W_{\text{ST}}(E_\lambda; T, \lambda) \\ &= \int dE_0 dV n(E_0, V) \exp(-\beta E_\lambda + f(T, \lambda)) = \text{const} . \end{aligned} \quad (99)$$

In the numerical work we discretize the parameter set in $M = N_T \times L$ different values, (T_I, λ_J) ($I = 1, \dots, N_T, J = 1, \dots, L$). Without loss of generality we can order the parameters so that $T_1 < T_2 < \dots < T_{N_T}$ and $\lambda_1 < \lambda_2 < \dots < \lambda_L$. The free energy f is now written as $f_{I,J} = f(T_I, \lambda_J)$. Once the initial configuration and the initial parameter set are chosen, the two-dimensional ST is then realized by alternately performing the following two steps:

1. A canonical MC or MD simulation at the fixed parameter set (T_I, λ_J) is carried out for a certain steps.
2. One of the parameters in the parameter set (T_I, λ_J) is updated to the neighboring values with the configuration and the other parameter fixed. The transition probability of this parameter-updating process is given by the following Metropolis criterion:

$$w(T_I \rightarrow T_{I\pm 1}) = \min \left(1, \frac{W_{\text{ST}}(E_{\lambda_J}; T_{I\pm 1}, \lambda_J)}{W_{\text{ST}}(E_{\lambda_J}; T_I, \lambda_J)} \right) = \min(1, \exp(-\Delta)) , \quad (100)$$

where

$$\Delta = (\beta_{I\pm 1} - \beta_I) E_{\lambda_J} - (f_{I\pm 1, J} - f_{I, J}) , \quad (101)$$

for T -update, and

$$w(\lambda_J \rightarrow \lambda_{J\pm 1}) = \min \left(1, \frac{W_{\text{ST}}(E_{\lambda_{J\pm 1}}; T_I, \lambda_{J\pm 1})}{W_{\text{ST}}(E_{\lambda_J}; T_I, \lambda_J)} \right) = \min(1, \exp(-\Delta)) , \quad (102)$$

where

$$\begin{aligned} \Delta &= \beta_I (E_{\lambda_{J\pm 1}} - E_{\lambda_J}) - (f_{I, J\pm 1} - f_{I, J}) \\ &= \beta_I (\lambda_{J\pm 1} - \lambda_J) V - (f_{I, J\pm 1} - f_{I, J}) , \end{aligned} \quad (103)$$

for λ -update.

Finally, we present the corresponding MREM. We prepare N_T temperatures and L λ parameters, which makes the total number of replicas $M = N_T \times L$. We perform the following replica-exchange processes alternately:

1. Exchange pairs of replicas corresponding to neighboring temperatures, T_I and T_{I+1} (We refer to this process as T -exchange.)
2. Exchange pairs of replicas corresponding to “neighboring” λ parameters, λ_J and λ_{J+1} (We refer to this process as λ -exchange.)

The acceptance criterion for these replica exchanges is given by Eq. (53), where Eq. (75) now reads

$$\Delta = (\beta_I - \beta_{I+1}) (E_{\lambda_J} (q^{[j]}) - E_{\lambda_J} (q^{[i]})) , \quad (104)$$

for T -exchange, and

$$\begin{aligned}\Delta &= \beta_I \left(E_{\lambda_J} \left(q^{[j]} \right) - E_{\lambda_J} \left(q^{[i]} \right) - E_{\lambda_{J+1}} \left(q^{[j]} \right) + E_{\lambda_{J+1}} \left(q^{[i]} \right) \right) \\ &= \beta_I \left(\lambda_J - \lambda_{J+1} \right) \left(V \left(q^{[j]} \right) - V \left(q^{[i]} \right) \right) ,\end{aligned}\tag{105}$$

for λ -exchange.

After a short MREM simulation, we can use the multiple-histogram reweighting techniques to obtain $n(E_0, V)$ and $f_{I,J}$. Let $N_{I,J}(E_0, V)$ and $n_{I,J}$ be respectively the potential-energy histogram and the total number of samples obtained for the parameter set (T_I, λ_J) . The WHAM equations are then given by

$$n(E_0, V) = \frac{\sum_{I=1}^{N_T} \sum_{J=1}^L N_{I,J}(E_0, V)}{\sum_{I=1}^{N_T} \sum_{J=1}^L n_{I,J} \exp(f_{I,J} - \beta_I E_{\lambda_J})} ,\tag{106}$$

and for each I and J ($I = 1, \dots, N_T, J = 1, \dots, L$)

$$\exp(-f_{I,J}) = \sum_{E_0, V} n(E_0, V) \exp(-\beta_I E_{\lambda_J}) .\tag{107}$$

These equations are solved self-consistently by iteration for $n(E_0, V)$ and $f_{I,J}$.

Hence, we can determine the multidimensional multicanonical weight factor $W_{\text{mu}}(E_0, V)$ and the multidimensional simulated tempering weight factor $W_{\text{ST}}(E_{\lambda_J}; T_I, \lambda_J)$. The former is given by

$$W_{\text{mu}}(E_0, V) = \frac{1}{n(E_0, V)} ,\tag{108}$$

and the latter is given by

$$W_{\text{ST}}(E_{\lambda_J}; T_I, \lambda_J) = \exp(-\beta_I E_{\lambda_J} + f_{I,J}) .\tag{109}$$

3 SIMULATION RESULTS

We first compare the performances of REM, MUCAREM, and REMUCA. The accuracy of average quantities calculated depend on the “quality” of the random walk in the potential energy space, and the measure for this quality can be given by the number of tunneling events [15, 94]. One tunneling event is defined by a trajectory that goes from E_H to E_L and back, where E_H and E_L are the values near the highest energy and the lowest energy, respectively, which the random walk can reach. If E_H is sufficiently high, the trajectory gets completely uncorrelated when it reaches E_H . On the other hand, when the trajectory reaches near E_L , it tends to get trapped in local-minimum states. We thus consider that the more tunneling events we observe during a fixed number of MC/MD steps, the more efficient the method is as a generalized-ensemble algorithm (or, the average quantities obtained by the reweighting techniques are more reliable).

The first example is Monte Carlo simulations of the system of a 17-residue fragment of ribonuclease T1 in implicit solvent (expressed by the solvent accessible surface area)

[94]. The amino-acid sequence is Ser-Ser-Asp-Val-Ser-Thr-Ala-Gln-Ile-Ala-Ala-Tyr-Lys-Leu-His-Glu-Asp. The energy function E_{TOT} that we used is the sum of the conformational energy term of the solute E_{P} and the solvation free energy term E_{SOL} for the interaction of the peptide with the surrounding solvent: $E_{\text{TOT}} = E_{\text{P}} + E_{\text{SOL}}$. Here, the solvation term E_{SOL} is given by the sum of the terms that are proportional to the solvent-accessible surface area of the atomic groups of the solute. The parameters in the conformational energy as well as the molecular geometry were taken from ECEPP/2. The parameters of the solvent term were adopted from Ref. [125]. The computer code KONF90 [126, 127] was used, and MC simulations based on the REM, MUCAREM, and REMUCA were performed. For the calculation of a solvent-accessible surface area, we used the computer code NSOL [128]. The dihedral angles ϕ and ψ in the main chain and χ in the side chain constituted the variables to be updated in the MC simulations. The number of degrees of freedom for the peptide is 80. One MC sweep consists of updating all these angles once with Metropolis evaluation for each update. The simulations were started from randomly generated conformations. In Table 1 we list the number of tunneling events in REM, MUCAREM, and REMUCA simulations of the same system [94].

Table 1: Number of tunneling events in the MC simulations of a fragment of ribonuclease T1 for REM, MUCAREM, and REMUCA simulations

Total MC sweeps	REM	MUCAREM	REMUCA
2×10^6	2	9	18
3×10^6	5	16	29
4×10^6	9	22	38

Table 2: Number of tunneling events in the MD simulations of three peptides in explicit water for REM, MUCAREM, and REMUCA simulations

Peptide	No. of atoms	Total MD steps	REMD	MUCAREM	REMUCA
Alanine dipeptide	418	4×10^6	11	40	59
Alanine trimer	876	5×10^6	1	20	29
Met-enkephalin	1662	8×10^6	0	12	27

Hence, REMUCA is the most efficient, then MUCAREM, and finally REM.

The next systems are small peptides in explicit water [129]. When we consider explicit water molecules, the problem becomes order-of-magnitude more difficult than the case with implicit water models. They are alanine dipeptide with 132 water molecules, alanine trimer with 278 water molecules, and Met-enkephalin with 526 water molecules. The force-field, or the potential energy, that we used is AMBER parm96 [130] for the peptides and TIP3P [131] for water molecules. The peptides were placed inside the spheres of water molecules and the harmonic constraining forces were imposed in order to prevent the water molecules from flying apart. The unit time step, Δt , was set to 0.5 fsec. The

modified version [132, 133] of the software PRESTO version 2 [134] was used. In Table 2 we list the number of tunneling events in these systems.

The last system is the C-peptide of ribonuclease A in explicit water [135]. In the model of simulations, the N-terminus and the C-terminus of the C-peptide analogue were blocked with the acetyl group and the N-methyl group, respectively. The number of amino acids is 13 and the amino-acid sequence is: Ace-Ala-Glu⁻-Thr-Ala-Ala-Ala-Lys⁺-Phe-Leu-Arg⁺-Ala-His⁺-Ala-Nme [136, 137]. The initial configuration of our simulation was first generated by a high temperature molecular dynamics simulation (at $T = 1000$ K) in gas phase, starting from a fully extended conformation. We randomly selected one of the structures that do not have any secondary structures such as α -helix and β -sheet. The peptide was then solvated in a sphere of radius 22 Å, in which 1387 water molecules were included (see Fig. 1). Harmonic restraint was applied to prevent the water molecules from going out of the sphere. The total number of atoms is 4365. The dielectric constant was set equal to 1.0. The force-field parameters for protein were taken from the all-atom version of AMBER parm99 [138], which was found to be suitable for studying helical peptides [139], and TIP3P model [131] was used for water molecules. The unit time step, Δt , was set to 0.5 fsec.

In Table 3 the essential parameters in the simulations performed in this article are summarized.

We first performed a REMD simulation with 32 replicas for 100 psec per replica (REMD1 in Table 3). During this REMD simulation, replica exchange was tried every 200 MD steps. Using the obtained potential-energy histogram of each replica as input data to the multiple-histogram analysis in Eqs. (4) and (5), we obtained the first estimate of the multicanonical weight factor, or the density of states. We divided this multicanonical weight factor into four multicanonical weight factors that cover different energy regions [88, 93, 94] and assigned these multicanonical weight factors into four replicas (the weight factors cover the potential energy ranges from -13791.5 to -11900.5 kcal/mol, from -12962.5 to -10796.5 kcal/mol, from -11900.5 to -9524.5 kcal/mol, and from -10796.5 to -8293.5 kcal/mol). We then carried out a MUCAREM simulation with four replicas for 1 nsec per replica (MUCAREM1 in Table 3), in which replica exchange was tried every 1000 MD steps. We again used the potential-energy histogram of each replica as the input data to the multiple-histogram analysis and finally obtained the multicanonical weight factor with high precision. As a production run, we carried out a 15 nsec multicanonical MD simulation with one replica (REMUCA1 in Table 3) and the results of this production run were analyzed in detail.

In Fig. 2 we show the probability distributions of potential energy that were obtained from the above three generalized-ensemble simulations, namely, REMD1, MUCAREM1, and REMUCA1. We see in Fig. 2(a) that there are enough overlaps between all pairs of neighboring canonical distributions, suggesting that there were sufficient numbers of replica exchange in REMD1. We see in Fig. 2(b) that there are good overlaps between all pairs of neighboring multicanonical distributions, implying that MUCAREM1 also performed properly. Finally, the multicanonical distribution in Fig. 2(c) is completely flat between around -13000 kcal/mol and around -8000 kcal/mol. The results suggest that a free random walk was realized in this energy range.

In Fig. 3a we show the time series of potential energy from REMUCA1. We indeed observe a random walk covering as much as 5000 kcal/mol of energy range (note that 23 kcal/mol ≈ 1 eV). We show in Fig. 3(b) the average potential energy as a function of

temperature, which was obtained from the trajectory of REMUCA1 by the reweighting techniques. The average potential energy monotonically increases as the temperature increases.

Here, we took $E_H = -8250$ kcal/mol and $E_L = -12850$ kcal/mol for the measurement of the tunneling events. The random walk in REMUCA1 yielded as many as 55 tunneling events in 15 nsec. The corresponding numbers of tunneling events for REMD1 and for MUCAREM1 were 0 in 3.2 nsec and 5 in 4 nsec, respectively. Hence, REMUCA is the most efficient and reliable among the three generalized-ensemble algorithms.

In Fig. 4 the potential of mean force (PMF), or free energy, along the first two principal component axes at 300 K is shown. There exist three distinct minima in the free-energy landscape, which correspond to three local-minimum-energy states. We show representative conformations at these minima in Fig. 5. The structure of the global-minimum free-energy state (GM) has a partially distorted α -helix with the salt bridge between Glu⁻-2 and Arg⁺-10. The structure is in good agreement with the experimental structure obtained by both NMR and X-ray experiments. In this structure there also exists a contact between Phe-8 and His⁺-12. This contact is again observed in the corresponding residues of the X-ray structure. At LM1 the structure has a contact between Phe-8 and His⁺-12, but the salt bridge between Glu⁻-2 and Arg⁺-10 is not formed. On the other hand, the structure at LM2 has this salt bridge, but it does not have a contact between Phe-8 and His⁺-12. Thus, only the structures at GM satisfy all of the interactions that have been observed by the X-ray and other experimental studies.

Finally, we remark that the largest peptide in explicit water that we have succeeded in folding into the native structure from random initial conformations is so far the 16-residue C-terminal β -hairpin of streptococcal protein G B1 domain, which was accomplished by MUCAREM simulations with eight replicas [142].

4 CONCLUSIONS

In this article we have reviewed some of powerful generalized-ensemble algorithms for both Monte Carlo simulations and molecular dynamics simulations. A simulation in generalized ensemble realizes a random walk in potential energy space, alleviating the multiple-minima problem that is a common difficulty in simulations of complex systems with many degrees of freedom.

Detailed formulations of the three well-known generalized-ensemble algorithms, namely, multicanonical algorithm (MUCA), simulated tempering (ST), and replica-exchange method (REM), were given.

We then introduced several new generalized-ensemble algorithms that combine the merits of the above three methods.

The question is then which method is the most recommended. Our criterion for the effectiveness of generalized-ensemble algorithms was how many random walk cycles (tunneling events) in potential energy space between the high-energy region and low-energy region are realized within a fixed number of total MC (or MD) steps. We found that once the optimal MUCA weight factor is obtained, MUCA (and REMUCA) is the most effective (i.e., has the most number of tunneling events), and REM is the least [93]. We also found that once the optimal ST weight factor is obtained, ST (and REST) has more tunneling events than REM [89, 115]. Moreover, we compared the efficiency

of Berg’s recursion [73], Wang-Landau method [23, 24], and REMUCA/MUCAREM as methods for the multicanonical weight factor determination in two-dimensional 10-state Potts model and found that the three methods are about equal in efficiency [143]–[145].

Hence, the answer to the above question will depend on how much time one is willing to (or forced to) spend in order to determine the MUCA or ST weight factors. Given a problem, the first choice is REM because of its simplicity (no weight factor determination is required). If REM turns out to be insufficient or too much time-consuming (like the case with first-order phase transitions), then other more powerful algorithms such as MUCAREM and STREM are recommended.

Acknowledgements:

This work was supported, in part, by Grants-in-Aid for Scientific Research in Priority Areas (“Water and Biomolecules” and “Membrane Interface”) and for the Next Generation Super Computing Project, Nanoscience Program from the Ministry of Education, Culture, Sports, Science and Technology (MEXT), Japan.

References

- [1] U.H.E. Hansmann, Y. Okamoto: Generalized-ensemble approach for protein folding simulations. In: *Annual Reviews of Computational Physics VI*, ed by D. Stauffer (World Scientific, Singapore, 1999) pp. 129–157.
- [2] A. Mitsutake, Y. Sugita, Y. Okamoto: *Biopolymers (Peptide Science)* **60**, 96–123 (2001).
- [3] Y. Sugita, Y. Okamoto: Free-energy calculations in protein folding by generalized-ensemble algorithms. In: *Lecture Notes in Computational Science and Engineering*, ed by T. Schlick, H.H. Gan (Springer-Verlag, Berlin, 2002) pp. 304–332; e-print: cond-mat/0102296.
- [4] B.A. Berg: *Comp. Phys. Commun.* **147**, 52–57 (2002).
- [5] Y. Okamoto: *J. Mol. Graphics Mod.* **22**, 425–439 (2004); e-print: cond-mat/0308360.
- [6] H. Kokubo, Y. Okamoto: *Mol. Sim.* **32**, 791–801 (2006).
- [7] S.G. Itoh, H. Okumura, Y. Okamoto: *Mol. Sim.* **33**, 47–56 (2007).
- [8] A.M. Ferrenberg, R.H. Swendsen: *Phys. Rev. Lett.* **61**, 2635–2638 (1988); *ibid.* **63**, 1658 (1989).
- [9] A.M. Ferrenberg, R.H. Swendsen: *Phys. Rev. Lett.* **63**, 1195–1198 (1989).
- [10] S. Kumar, D. Bouzida, R.H. Swendsen, P.A. Kollman, J.M. Rosenberg: *J. Comput. Chem.* **13**, 1011–1021 (1992).
- [11] R.H. Swendsen, J.S. Wang: *Phys. Rev. Lett.* **58**, 86–88 (1987).

- [12] U. Wolff: Phys. Rev. Lett. **62**, 361–364 (1989).
- [13] H.G. Evertz, G. Lana, M. Marcu: Phys. Rev. Lett. **70**, 875–879 (1993).
- [14] B.A. Berg, T. Neuhaus: Phys. Lett. **B267**, 249–253 (1991).
- [15] B.A. Berg, T. Neuhaus, Phys. Rev. Lett. **68**, 9–12 (1992).
- [16] B.A. Berg: *Fields Institute Communications* **26**, 1–24 (2000); also see e-print: cond-mat/9909236.
- [17] W. Janke: Physica A **254**, 164–178 (1998).
- [18] J. Lee: Phys. Rev. Lett. **71**, 211–214 (1993); *ibid.* **71**, 2353 (1993).
- [19] M. Mezei: J. Comput. Phys. **68**, 237–248 (1987).
- [20] C. Bartels, M. Karplus: J. Phys. Chem. B **102**, 865–880 (1998).
- [21] G.M. Torrie, J.P. Valleau: J. Comput. Phys. **23**, 187–199 (1977).
- [22] J.S. Wang, R.H. Swendsen: J. Stat. Phys. **106**, 245–285 (2002).
- [23] F. Wang, D.P. Landau: Phys. Rev. Lett. **86**, 2050–2053 (2001).
- [24] F. Wang, D.P. Landau: Phys. Rev. E **64**, 056101 (2001).
- [25] Q. Yan, R. Faller, J.J. de Pablo: J. Chem. Phys. **116**, 8745–8749 (2002).
- [26] S. Trebst, D.A. Huse, M. Troyer: Phys. Rev. E **70** 046701 (2004).
- [27] B.A. Berg, T. Celik: Phys. Rev. Lett. **69**, 2292–2295 (1992).
- [28] B.A. Berg, U.H.E. Hansmann, T. Neuhaus: Phys. Rev. B **47**, 497–500 (1993).
- [29] W. Janke, S. Kappler: Phys. Rev. Lett. **74**, 212–215 (1995). **74**,
- [30] B.A. Berg, W. Janke: Phys. Rev. Lett. **80**, 4771–4774 (1998).
- [31] N. Hatano, J.E. Gubernatis: Prog. Theor. Phys. (Suppl.) **138**, 442–447 (2000).
- [32] B.A. Berg, A. Billoire, W. Janke: Phys. Rev. B **61**, 12143–12150 (2000).
- [33] U.H.E. Hansmann, Y. Okamoto: J. Comput. Chem. **14**, 1333–1338 (1993).
- [34] U.H.E. Hansmann, Y. Okamoto: Physica **A212**, 415–437 (1994).
- [35] M.H. Hao, H.A. Scheraga: J. Phys. Chem. **98**, 4940–4948 (1994).
- [36] Y. Okamoto, U.H.E. Hansmann: J. Phys. Chem. **99**, 11276–11287 (1995).
- [37] N.B. Wilding: Phys. Rev. E **52**, 602–611 (1995).
- [38] A. Kolinski, W. Galazka, J. Skolnick: *Proteins* **26**, 271–287 (1996).
- [39] N. Urakami, M. Takasu: J. Phys. Soc. Jpn. **65**, 2694–2699 (1996).

- [40] S. Kumar, P. Payne, M. Vásquez: *J. Comput. Chem.* **17**, 1269–1275 (1996).
- [41] U.H.E. Hansmann, Y. Okamoto, F. Eisenmenger: *Chem. Phys. Lett.* **259**, 321–330 (1996).
- [42] U.H.E. Hansmann, Y. Okamoto: *Phys. Rev. E* **54**, 5863–5865 (1996).
- [43] U.H.E. Hansmann, Y. Okamoto: *J. Comput. Chem.* **18**, 920–933 (1997).
- [44] N. Nakajima, H. Nakamura, A. Kidera: *J. Phys. Chem. B* **101**, 817–824 (1997).
- [45] C. Bartels, M. Karplus: *J. Comput. Chem.* **18**, 1450–1462 (1997).
- [46] J. Higo, N. Nakajima, H. Shirai, A. Kidera, H. Nakamura: *J. Comput. Chem.* **18**, 2086–2092 (1997).
- [47] Y. Iba, G. Chikenji, M. Kikuchi: *J. Phys. Soc. Jpn.* **67**, 3327–3330 (1998).
- [48] A. Mitsutake, U.H.E. Hansmann, Y. Okamoto: *J. Mol. Graphics Mod.* **16**, 226–238; 262–263 (1998).
- [49] U.H.E. Hansmann, Y. Okamoto: *J. Phys. Chem. B* **103**, 1595–1604 (1999).
- [50] H. Shimizu, K. Uehara, K. Yamamoto, and Y. Hiwatari: *Mol. Sim.* **22**, 285–301 (1999).
- [51] S. Ono, N. Nakajima, J. Higo, H. Nakamura: *Chem. Phys. Lett.* **312**, 247–254 (1999).
- [52] A. Mitsutake, Y. Okamoto: *J. Chem. Phys.* **112**, 10638–10647 (2000).
- [53] K. Sayano, H. Kono, M.M. Gromiha, and A. Sarai: *J. Comput. Chem.* **21**, 954–962 (2000).
- [54] F. Yasar, T. Celik, B.A. Berg, H. Meirovitch: *J. Comput. Chem.* **21**, 1251–1261 (2000).
- [55] A. Mitsutake, M. Kinoshita, Y. Okamoto, F. Hirata: *Chem. Phys. Lett.* **329**, 295–303 (2000).
- [56] M.S. Cheung, A.E. Garcia, J.N. Onuchic: *Proc. Natl. Acad. Sci. U.S.A.* **99**, 685–690 (2002).
- [57] N. Kamiya, J. Higo, H. Nakamura: *Protein Sci.* **11**, 2297–2307 (2002).
- [58] S.W. Jang, Y. Pak, S.M. Shin: *J. Chem. Phys.* **116**, 4782–4786 (2002).
- [59] J.G. Kim, Y. Fukunishi, H. Nakamura: *Phys. Rev. E* **67**, 011105 (2003).
- [60] N. Rathore, T.A. Knotts, IV, J.J. de Pablo: *J. Chem. Phys.* **118**, 4285–4290 (2003).
- [61] T. Terada, Y. Matsuo, A. Kidera: *J. Chem. Phys.* **118**, 4306–4311 (2003).

- [62] B.A. Berg, H. Noguchi, Y. Okamoto: Phys. Rev. E **68**, 036126 (2003).
- [63] M. Bachmann, W. Janke: Phys. Rev. Lett. **91**, 208105 (2003).
- [64] H. Okumura, Y. Okamoto: Chem. Phys. Lett. **383**, 391–396 (2004).
- [65] T. Munakata, S. Oyama: Phys. Rev. E **54**, 4394–4398 (1996).
- [66] A.P. Lyubartsev, A.A. Martinovski, S.V. Shevkunov, P.N. Vorontsov-Velyaminov: J. Chem. Phys. **96**, 1776–1783 (1992).
- [67] E. Marinari, G. Parisi: Europhys. Lett. **19**, 451–458 (1992).
- [68] E. Marinari, G. Parisi, J.J. Ruiz-Lorenzo: In: *Spin Glasses and Random Fields*, ed by A.P. Young (World Scientific, Singapore, 1998) pp. 59–98.
- [69] A. Irbäck, F. Potthast: J. Chem. Phys. **103**, 10298–10305 (1995).
- [70] A. Irbäck, E. Sandelin: J. Chem. Phys. **110**, 12256–12262 (1999).
- [71] G.R. Smith, A.D. Bruce: Phys. Rev. E **53**, 6530–6543 (1996).
- [72] U.H.E. Hansmann: Phys. Rev. E **56**, 6200–6203 (1997).
- [73] B.A. Berg: Nucl. Phys. B (Proc. Suppl.) **63A-C**, 982–984 (1998).
- [74] W. Janke: Histograms and all that. In: *Computer Simulations of Surfaces and Interfaces V*, NATO Science Series, II Mathematics, Physics and Chemistry Vol. **114**, Proceedings of the NATO Advanced Study Institute, ed by B. Dünweg, D.P. Landau, A.I. Milchev (Kluwer, Dordrecht, 2003), pp. 137–157.
- [75] K. Hukushima, K. Nemoto: J. Phys. Soc. Jpn. **65**, 1604–1608 (1996).
- [76] K. Hukushima, H. Takayama, K. Nemoto: Int. J. Mod. Phys. C **7**, 337–344 (1996).
- [77] C.J. Geyer: In: *Computing Science and Statistics: Proc. 23rd Symp. on the Interface*, ed by E.M. Keramidas (Interface Foundation, Fairfax Station, 1991) pp. 156–163.
- [78] R.H. Swendsen, J.-S. Wang: Phys. Rev. Lett. **57**, 2607–2609 (1986).
- [79] K. Kimura, K. Taki: In: *Proc. 13th IMACS World Cong. on Computation and Appl. Math. (IMACS '91)*, ed by R. Vichnevetsky, J.J.H. Miller, vol. 2, pp. 827–828.
- [80] D.D. Frantz, D.L. Freeman, J.D. Doll: J. Chem. Phys. **93**, 2769–2784 (1990).
- [81] M.C. Tesi, E.J.J. van Rensburg, E. Orlandini, S.G. Whittington: J. Stat. Phys. **82**, 155–181 (1996).
- [82] Y. Iba: Int. J. Mod. Phys. C **12**, 623–656 (2001).
- [83] U.H.E. Hansmann: Chem. Phys. Lett. **281**, 140–150 (1997).

- [84] Y. Sugita, Y. Okamoto: Chem. Phys. Lett. **314**, 141–151 (1999).
- [85] M.G. Wu, M.W. Deem: Mol. Phys. **97**, 559–580 (1999).
- [86] Y. Sugita, A. Kitao, Y. Okamoto: J. Chem. Phys. **113**, 6042–6051 (2000).
- [87] C.J. Woods, J.W. Essex, M.A. King: J. Phys. Chem. B **107**, 13703–13710 (2003).
- [88] Y. Sugita, Y. Okamoto: Chem. Phys. Lett. **329**, 261–270 (2000).
- [89] A. Mitsutake, Y. Okamoto: Chem. Phys. Lett. **332**, 131–138 (2000).
- [90] D. Gront, A. Kolinski, J. Skolnick: J. Chem. Phys. **113**, 5065–5071 (2000).
- [91] G.M. Verkhivker, P.A. Rejto, D. Bouzida, S. Arthurs, A.B. Colson, S.T. Freer, D.K. Gehlhaar, V. Larson, B.A. Luty, T. Marrone, P.W. Rose: Chem. Phys. Lett. **337**, 181–189 (2001).
- [92] H. Fukunishi, O. Watanabe, S. Takada: J. Chem. Phys. **116**, 9058–9067 (2002).
- [93] A. Mitsutake, Y. Sugita, Y. Okamoto: J. Chem. Phys. **118**, 6664–6675 (2003).
- [94] A. Mitsutake, Y. Sugita, Y. Okamoto: J. Chem. Phys. **118**, 6676–6688 (2003).
- [95] A. Sikorski, P. Romiszowski: Biopolymers **69**, 391–398 (2003).
- [96] C.Y. Lin, C.K. Hu, U.H.E. Hansmann: Proteins **52**, 436–445 (2003).
- [97] G. La Penna, A. Mitsutake, M. Masuya, Y. Okamoto: Chem. Phys. Lett. **380**, 609–619 (2003).
- [98] M. Falcioni, M.W. and Deem, M.W. (1999) J. Chem. Phys. **110**, 1754–1766.
- [99] Q. Yan, J.J. de Pablo: J. Chem. Phys. **111**, 9509–9516 (1999).
- [100] T. Nishikawa, H. Ohtsuka, Y. Sugita, M. Mikami, Y. Okamoto: Prog. Theor. Phys. (Suppl.) **138**, 270–271 (2000).
- [101] R. Yamamoto, W. Kob: Phys. Rev. E **61**, 5473–5476 (2000).
- [102] D.A. Kofke: J. Chem. Phys. **117**, 6911–6914 (2002).
- [103] T. Okabe, M. Kawata, Y. Okamoto, M. Mikami: Chem. Phys. Lett. **335**, 435–439 (2001).
- [104] Y. Ishikawa, Y. Sugita, T. Nishikawa, Y. Okamoto: Chem. Phys. Lett. **333**, 199–206 (2001).
- [105] A.E. Garcia, K.Y. Sanbonmatsu: Proteins **42**, 345–354 (2001).
- [106] R.H. Zhou, B.J. Berne, R. Germain: Proc. Natl. Acad. Sci. U.S.A. **98**, 14931–14936 (2001).
- [107] A.E. Garcia, K.Y. Sanbonmatsu: Proc. Natl. Acad. Sci. U.S.A. **99**, 2782–2787 (2002).

- [108] R.H. Zhou, B.J. Berne: *Proc. Natl. Acad. Sci. U.S.A.* **99**, 12777–12782 (2002).
- [109] M. Feig, A.D. MacKerell, C.L. Brooks, III: *J. Phys. Chem. B* **107**, 2831–2836 (2003).
- [110] Y.M. Rhee, V.S. Pande: *Biophys. J.* **84**, 775–786 (2003).
- [111] J.W. Pitera, W. Swope: *Proc. Natl. Acad. Sci. U.S.A.* **100**, 7587–7592 (2003).
- [112] M.K. Fenwick, F.A. Escobedo: *Biopolymers* **68**, 160–177 (2003).
- [113] H.F. Xu, B.J. Berne: *J. Chem. Phys.* **112**, 2701–2708 (2000).
- [114] R. Faller, Q. Yan, J.J. de Pablo: *J. Chem. Phys.* **116**, 5419–5423 (2002).
- [115] A. Mitsutake, Y. Okamoto: *J. Chem. Phys.* **121**, 2491–2504 (2004).
- [116] M.K. Fenwick, F.A. Escobedo: *J. Chem. Phys.* **119**, 11998–12010 (2003).
- [117] K. Hukushima: *Phys. Rev. E* **60**, 3606–3614 (1999).
- [118] T.W. Whitfield, L. Bu, J.E. Straub: *Physica A* **305**, 157–171 (2002).
- [119] W. Kwak, U.H.E. Hansmann: *Phys. Rev. Lett.* **95**, 138102 (2005).
- [120] N. Metropolis, A.W. Rosenbluth, M.N. Rosenbluth, A.H. Teller, E. Teller: *J. Chem. Phys.* **21**, 1087–1092 (1953).
- [121] S. Nosé: *Mol. Phys.* **52**, 255–268 (1984).
- [122] S. Nosé: *J. Chem. Phys.* **81**, 511–519 (1984).
- [123] B.A. Berg: *Markov Chain Monte Carlo Simulations and Their Statistical Analysis* (World Scientific, Singapore, 2004) p. 253.
- [124] B.A. Berg: *Comp. Phys. Commun.* **153**, 397–406 (2003).
- [125] T. Ooi, M. Oobatake, G. Némethy, H.A. Scheraga: *Proc. Natl. Acad. Sci. USA* **84**, 3086–3090 (1987).
- [126] H. Kawai, Y. Okamoto, M. Fukugita, T. Nakazawa, T. Kikuchi: *Chem. Lett.* **1991**, 213–216 (1991).
- [127] Y. Okamoto, M. Fukugita, T. Nakazawa, H. Kawai: *Protein Eng.* **4**, 639–647 (1991).
- [128] M. Masuya, manuscript in preparation; see also <http://biocomputing.cc/nsol/>.
- [129] Y. Sugita, Y. Okamoto: unpublished.
- [130] P.A. Kollman, R. Dixon, W. Cornell, T. Fox, C. Chipot, A. Pohorille: in *Computer Simulation of Biomolecular Systems Vol. 3*, ed by A. Wilkinson, P. Weiner, W.F. van Gunsteren (Kluwer, Dordrecht, 1997) pp. 83–96.

- [131] W.L. Jorgensen, J. Chandrasekhar, J.D. Madura, R.W. Impey, M.L. Klein: *J. Chem. Phys.* **79**, 926–935 (1983).
- [132] Y. Sugita, A. Kitao: *Proteins* **30**, 388–400 (1998).
- [133] A. Kitao, S. Hayward, N. Gō: *Proteins* **33**, 496–517 (1998).
- [134] K. Morikami, T. Nakai, A. Kidera, M. Saito, H. Nakamura: *Comp. Chem.* **16**, 243–248 (1992).
- [135] Y. Sugita, Y. Okamoto: *Biophys. J.* **88**, 3180–3190 (2005).
- [136] K.R. Shoemaker, P.S. Kim, E.J. York, J.M. Stewart, R.L. Baldwin: *Nature* **326**, 563–567 (1987).
- [137] K.R. Shoemaker, R. Fairman, D.A. Schultz, A.D. Robertson, E.J. York, J.M. Stewart, R.L. Baldwin: *Biopolymers* **29**, 1–11 (1990).
- [138] J. Wang, P. Cieplak, P.A. Kollman: *J. Comput. Chem.* **21**, 1049–1074 (2000).
- [139] T. Yoda, Y. Sugita, Y. Okamoto: *Chem. Phys. Lett.* **386**, 460–467 (2004).
- [140] P.J. Kraulis: *J. Appl. Crystallogr.* **24**, 946–950 (1991).
- [141] E.A. Merritt, D.J. Bacon: *Methods Enzymol.* **277**, 505–524 (1997).
- [142] T. Yoda, Y. Sugita, Y. Okamoto: *Proteins* **66**, 846–859 (2007).
- [143] T. Nagasima, Y. Sugita, A. Mitsutake, Y. Okamoto: in preparation.
- [144] T. Nagasima, Y. Sugita, A. Mitsutake, Y. Okamoto: *Comp. Phys. Commun.* **146**, 69–76 (2002).
- [145] Y. Okamoto: Metropolis algorithms in generalized ensemble. In: *The Monte Carlo Method in the Physical Sciences: Celebrating the 50th Anniversary of the Metropolis Algorithm*, ed by J.E. Gubernatis (American Institute of Physics, Melville, 2003) pp. 248–260; e-print: cond-mat/0308119.

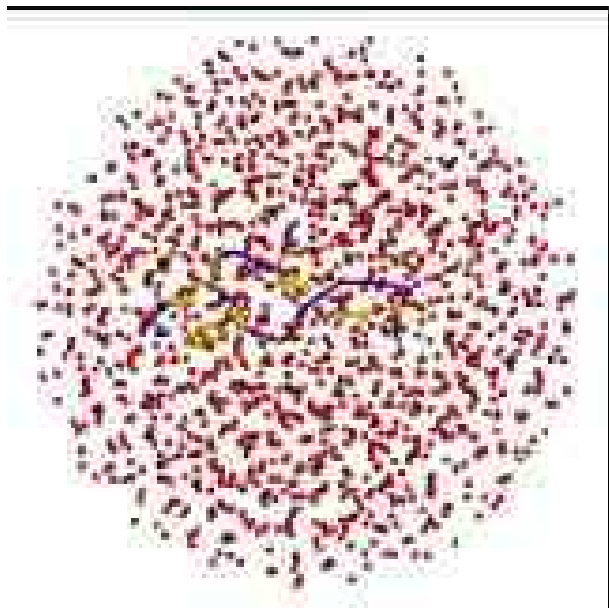


Figure 1: The initial configuration of C-peptide in explicit water, which was used in all of the 32 replicas of the first REMD simulation (REMD1 in Table 3). The red filled circles stand for the oxygen atoms of water molecules. The number of water molecules is 1387, and they are placed in a sphere of radius 22 Å. As for the peptide, besides the backbone structure (in blue), side chains of only Glu⁻-2, Phe-8, Arg⁺-10, and His⁺-12 are shown (in yellow). The figure was created with Molscript [140] and Raster3D [141].

Table 3: Summary of parameters in REMD, MUCAREM, and REMUCA simulations

	Number of replicas, M	Temperature, T_m (K) ($m = 1, \dots, M$)	MD steps per replica
REMD1*	32	250, 258, 267, 276, 286, 295, 305, 315, 326, 337, 348, 360, 372, 385, 398, 411, 425, 440, 455, 470, 486, 502, 519, 537, 555, 574, 593, 613, 634, 655, 677, 700	2.0×10^5
MUCAREM1	4	360, 440, 555, 700	2.0×10^6
REMUCA1	1	700	3.0×10^7

* REMD1 stands for the replica-exchange molecular dynamics simulation, MUCAREM1 stands for the multicanonical replica-exchange molecular dynamics simulation, and REMUCA1 stands for the final multicanonical molecular dynamics simulation (the production run) of REMUCA. The results of REMD1 were used to determine the multicanonical weight factors for MUCAREM1, and those of MUCAREM1 were used to determine the multicanonical weight factor for REMUCA1.

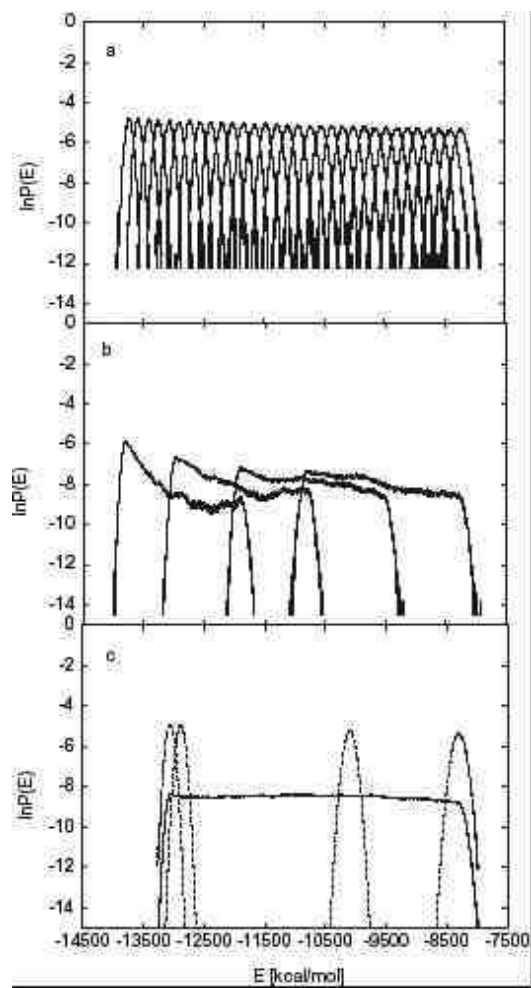


Figure 2: Probability distributions of potential energy of the C-peptide system obtained from (a) REMD1, (b) MUCAREM1, and (c) REMUCA1. See Table 3 for the parameters of the simulations. Dashed curves in (c) are the reweighted canonical distributions at 290, 300, 500, and 700 K (from left to right).

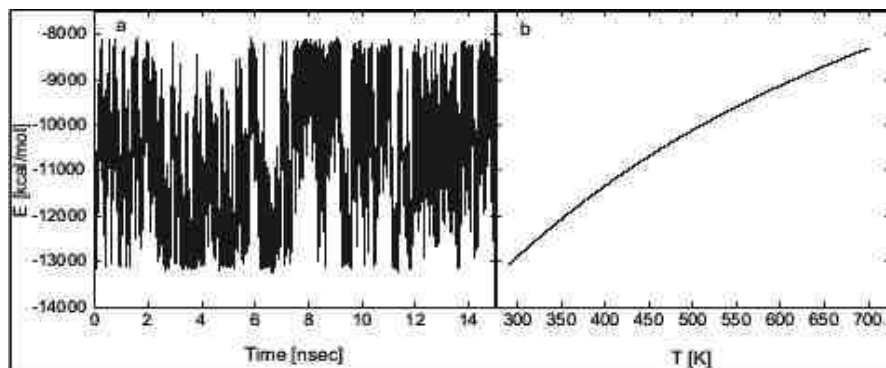


Figure 3: Time series of potential energy of the C-peptide system from the REMUCA production run (REMUCA1 in Table 3) (a) and the average potential energy as a function of temperature (b). The latter was obtained from the trajectory of REMUCA1 by the single-histogram reweighting techniques.

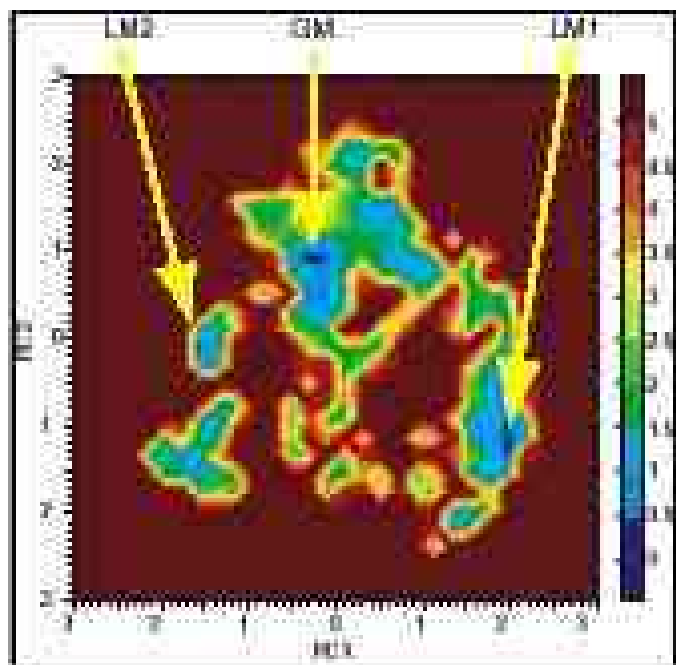


Figure 4: Potential of mean force (kcal/mol) of the C-peptide system along the first two principal components at 300 K. The free energy was calculated from the results of REMUCA production run (REMUCA1 in Table 3) by the single-histogram reweighting techniques and normalized so that the global-minimum state (GM) has the value zero. GM, LM1, and LM2 represent three distinct minimum free-energy states.

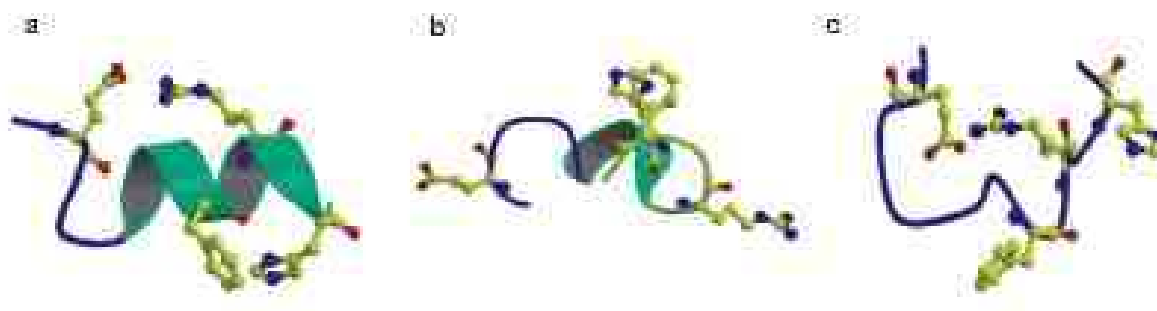


Figure 5: The representative structures at the global-minimum free-energy state ((a) GM) and the two local-minimum states ((b) LM1 and (c) LM2). As for the peptide structures, besides the backbone structure, side chains of only Glu⁻-2, Phe-8, Arg⁺-10, and His⁺-12 are shown in ball-and-stick model.